The Application of EM38: Determination of Soil Parameters, Selection of Soil Sampling Points and Use in Agriculture and Archaeology

Kurt Heil * and Urs Schmidhalter

Chair of Plant Nutrition, Technical University of Munich, D-85350 Freising, Emil-Ramann-Str. 2, Germany; schmidhalter@wzw.tum.de

* Correspondence: kheil@wzw.tum.de; Tel.: +49-8161-713-906

Abstract: Fast and accurate assessment of within-field variation is essential for detecting field-wide heterogeneity and contributing to improvements in the management of agricultural lands. The goal of this paper is to provide an overview of field scale characterization by electromagnetic induction, firstly with a focus on the applications of EM38 to salinity, soil texture, water content and soil water turnover, soil types and boundaries, nutrients and N-turnover and soil sampling designs. Furthermore, results concerning special applications in agriculture, horticulture and archaeology are included. In addition to these investigations, this survey also presents a wide range of practical methods for use. Secondly, the effectiveness of conductivity readings for a specific target in a specific locality is determined by the intensity at which soil factors influence these values in relationship to the desired information. The interpretation and utility of apparent electrical conductivity (EC_a) readings are highly location- and soil-specific, so soil properties influencing the measurement of EC_a must be clearly understood. From the various calibration results, it appears that regression constants for the relationships between EC_a, electrical conductivity of aqueous soil extracts (EC_e), texture, yield, etc., are not necessarily transferable from one region to another. The modelling of EC_a, soil properties, climate and yield are important for identifying the location to which specific utilizations of EC_a technology (e.g., EC_a–texture relationships) can be appropriately applied. In general, the determination of absolute levels of EC_a is frequently not possible, but it appears to be quite a robust method to detect relative differences, both spatially and temporally. Often, the use of EC_a is restricted to its application as a covariate or the use of the readings in a relative sense rather than as absolute terms.

Keywords: EM38; apparent electrical conductivity; soil mapping; yield variability and management zones; soil sampling schemes; soil types

1. Introduction

Fast and accurate detection of within-field variation is essential for the detection and management of the environment. The EM38 device (Geonics. Ltd., Mississauga, ON, Canada), a sensor that delivers dense datasets, can be used to accomplish this goal. The EM38 meter is the most widely used EMI sensor in agriculture [1,2].

Researchers have related EM38-EC_a (apparent electrical conductivity—EC_a) to a number of different soil properties either within an individual field or across the entire landscape [3]. The application of EM38 began with the detection of salinity and continued with the determination of clay and water content [2]. Currently, areas of application include the estimation of nutrient levels and other soil chemical and physical properties, soil sampling points, the determination of soil types and their boundaries, the prediction of yield and the delineation of crop management zones. The

increasing application especially during the last decade is also caused by various technical developments: Global Positioning Systems (GPS), surface mapping programs and systems for data analysis and interpretation. Technical data, construction and tool specification are described in Heil and Schmidhalter [4].

This device consists of a receiver and a transmitter coil installed 1.0 m apart at the opposite ends of a nonconductive bar. The investigated depth range depends on the coil configuration and the distance between the coils. While the distance is fixed, the orientation of the coils can be changed. In the vertical mode, the device is in a position perpendicular to the soil, whereas in the second case, the device lies parallel to the soil surface [5,6]. The sensitivity in the horizontal mode is the highest directly below the instrument, while the sensitivity in the vertical position reaches a maximum at approximately 30–40 cm below the instrument. The depth-weighted nonlinearity of the response is shown in Figure 1. The cumulative relative contributions of all soil EC are R(z).
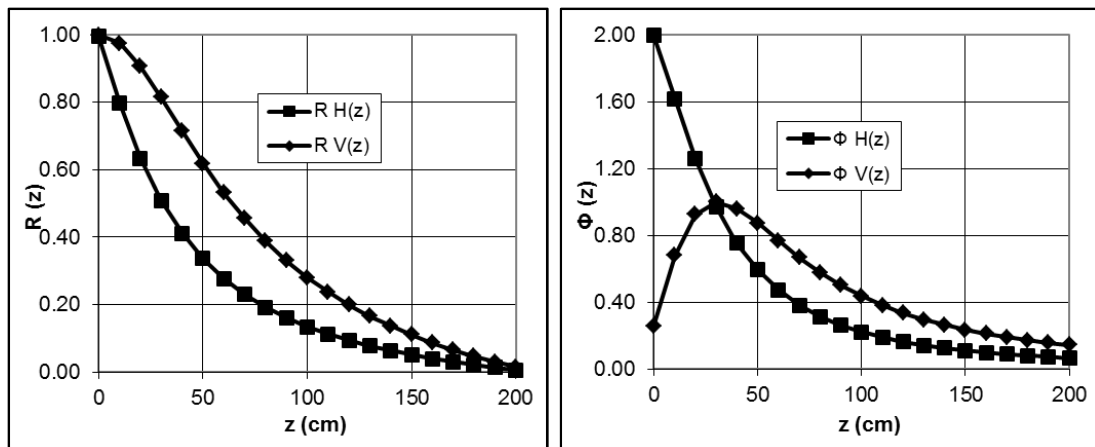

Figure 1. (**Left**) Relative cumulative contribution vs depth for vertically (RV(*z*)) and horizontally (RH(*z*)) orientated dipoles; (**Right**) Comparison of the relative responses for vertically (FV(*z*)) and horizontally (FH(*z*)) oriented dipoles.

An exact determination of the measurement depth is difficult. Theoretically, the readings acquire an unlimited depth, but in reality, it depends on the electrical contrast. The most common definition is a depth range up to 1.5 m when using the vertical dipole mode and 0.75 m in the case of the horizontal mode [4–6].

For wide area measurements e.g., in precision agriculture as well as in field-scale soil property measurements the sensor is mounted on metal-free sledge and pulled behind an all-terrain vehicle equipped with a GPS receiver and data collection computer (Figure 2).

Figure 2. Mounting of the EM38 on a metal-free sledge pulled by a tractor (constructed after Corwin and Lesch [7]).

Beside the EM38, EM31 and EM34 electromagnetic devices are also available on the market. In contrast to the EM38, the other devices are designed for the detection of deeper areas of soils, e.g., geological layers, ground water and other subsurface feature associated with changes in ground

conductivity. The EM31 has an effective exploration depth of about six metres with an intercoil spacing of 3.66 m. The EM34-3 uses three intercoil spacings—10, 20 and 40 m—to provide variable depths of exploration down to 60 metres.

2. Goal of this Study

The objective of this study is to summarize the results of recent measurements and the development of algorithms from EC_a measurements obtained with the geophysical sensor EM38. Given the numerous possible subject matters for research in using EM38, this review paper has focused on the following specific fields:

1. Salinity
2. Soil-related properties in non-saline soils
   - Soil texture
   - Soil water content, water balance
   - Soil horizons and vertical discontinuities
   - N-turnover, cation exchange capacity, organic matter and additional soil parameters
   - Soil sampling designs
   - Soil type boundaries
3. Agriculture
   - Agricultural yield variability and management zones
   - Efficiency of agricultural field experimentation
   - Additional application of EM38 in agriculture and horticulture
4. Archaeology

The rationale of this compilation should allow the users of this sensor to understand which variables are today detectable, which objectives are realistic and in which regions applications are widely used. The users have to note that these sensor readings are a composite of soil properties and therefore not a replacement for in-depth knowledge's about soil and site.

3. Surveying Soil Salinity

Ample information can be found in the literature that describes the potential of EM-38 measurements for the non-invasive detection of in situ soil salinity (Table 1).

Table 1. Overview with literature of relationships between EM38-EC_a and salinity.

Study	Parameters	Location of Investigation
	Derivation of salinity with EC_a and EC_e	
[8]	EC_a and EC_e relationships: classifying salt affected area	California, USA
[9]	Descriptions and formulations of EC_e and EC_a; mathematical coefficients;	South Australia
[10,11]	Descriptions and formulations of EC_e and EC_a; inverted salinity profiles;	South California, USA
[12]	EC_a and $EC_{saturated\ extract}$, Na, Cl, Salinity maps with relation to yield Barley)	North-east Australia
[13]	Calibration EC_e and EC_{av}, EC_{ah}	Missouri, USA
[14]	EC_a and $EC_{1:5}$ relationships to perform growth of Australian tree species on saline sites	Queensland, Australia
[15]	Formulations of EC_e and EC_a	Egypt
[16]	Relationship EC_a and EC_e, EC_a observations on establishing and growth of perennial pasture species	Australia
[17]	Salinity contour maps with EC_e and EC_{av}, EC_{ah}	Nnortheast Spain
[18]	Salinity classification system based on $EC_{1:5}$ with groups of degrades	Henan, China
[19]	Formulations of EC_e and EC_a	California, USA

Table 1. *Cont*.

[20]	EC_a, EC_e to apply site specific management tech. on saline sites	California, USA
[21]	EC_e and EC_{av}, EC_{ah} advanced calibrations reduce soil sampling from 200-300 to 36,	California, USA
[5,22]	Site calibration EC_e and EC_{av}, EC_{ah}	Saskatchewan, Canada
[23–26]	Formulations of EC_a and EC_e; Salt tolerance of trees, forages, crops and turf grasses; survival and growth of eucalyptus and pastures in saline soils.	Alberta, Canada
[27]	Exchangeable sodium percentage and EC_e in relation to EC_a	Illinois, USA
[28]	Soil survey with salinity regions; relationship EC_e and EC_a to detect salinity of irrigated districts	Aragon, Spain
[29]	Ranges of EC_a as classification system of saline areas	Victoria, Australia
[30]	Salinity classification system based on ranges of total dissolved salt concentrations, $EC_{1:5}$ with groups of crops with different tolerances to rootzone salinity	Victoria, Australia
[31–34]	Descriptions and formulations of EC_a, EC_e, EC_P and EC ratios; multiple regression coefficients;	California, USA
[35]	Relationships of EC_e and EC_a, Soil salinity maps of different depth intervals and salinity profile maps at upstream and downstream of the field borders	Yazd Province, Iran
[36]	Monitoring spill of liquid manure occurred a few years ago	Manitoba, Canada
[37]	Formulations of EC_e and EC_a (India)	India (different regions)
[38,39]	Descriptions and formulations of EC_e and EC_a; modeled coefficients;	NSW, Australia
[40]	Comparison $EC_{1:5}$ - EC_e and EC_a to detect salinity in an early stage	Nakhon Ratchasima, Thailand
[41]	Comparison EC_e and EC_a to detect salinity	New Mexico, USA
[42–45]	Determination EC_e profiles with EC_a (EM38 and EM31); geostatistical methods to predict salinity from EC_a (EM38 and EM31), comparison calibration approaches;	NSW, Queensland, Australia
[46,47]	Ratio (EM38/EM31) sampling points to determine deep drainage and leaching fraction, EC_a and EC_e; EC_a and clay; EC_a and deep drainage;	NSW, Australia
[48]	EC_e, water content and EC_{ah}, combined with cokriging	California, USA
[49]	Descriptions, formulations, classifications of EC_a, EC_e, EC_P and EC ratios	–
[50]	Overview salinity and determination	–
[51–53]	Detection subsurface saline material	Victoria, Australia
[54]	Calibration models EC_e and EC_a and water content over regional scale	Colorado, USA
[55]	Descriptions and formulations of EC_e and EC_a, simple depth weighted coefficients;	North Dakota, USA
[56]	Depthwise calibration models EC_{av}, EC_{ah} and EC_e and $EC_{1:5}$ to construct inverted salinity profiles	Jiangsu, China
[57]	Comparison saturated paste and 1:1 soil to water extracts	Oklahoma, Texas, USA
[58]	Formulations of EC_e and EC_a	Pakistan
[59]	Site calibration EC_e and EC_{av}, EC_{ah}	Navarre, Spain
[60]	Site calibration EC_e and EC_{av}, EC_{ah}	North Dakota, USA
[61]	Site calibration $EC_{(1:5)}$ and EC_{ah}	West Australia
[62]	Salinity calibration model to simulate EC_e from EC_a	California, Minnesota, USA
[57]	Comparison saturated paste and 1:1 soil to water extracts	Oklahoma, Texas, USA

Table 1. *Cont.*

	Construction of salinity maps	
[63]	Interpolation methods of EC_a; EC_a maps as base for salinity maps/EC_e)	Uzbekistan
[64]	Relation ECa-topography-salinity extension	Senegal
[65]	EC_a-salinity areas	SE Australia
[66]	Salinity maps with stepwise data processing	Victoria, Australia
[67]	Mapping salinity with EM38, EM31 and Wenner array	Alberta, Canada
[68]	Geostatistical analysis of soil salinity data	———
[69]	Salinity distribution within a field and combination with iodine tracer study	Cape Province, South Africa
[70]	Soil salinity maps with EC_a, in relation to land use and soil/geology	South Australia
[71]	EC_a and visual agronomic survey of salinity	Punjab, Pakistan
[72]	Mapping of salinity plume in a sandy aquifer	North Dakota, USA
[73]	Detecting salt stores and evaluation of the risk of salinisation	NSW, Australia
[74]	EC_a maps by inverting data collected at various heights in the EM4SOIL software	Yazd Province, Iran
[75]	Salinity characteristics with PCA	California, USA
[76]	Comparison of multiple linear regression and cokriging	California, USA
[77]	Temporal changes in salinity using EC_a	Aragon, Spain
[78–80]	Saline seep mapping and remediation; comparison salinity (EC_e) and EC_a of different conductivity tools; saline seep mechanism in combination with hydrological modeling	Kansas, USA
[81]	Comparison salinity (EC_a) between different land use	Australia
[82]	EM38 field wise	NSW, Australia
	Salinity and field management	
[83]	Assessment of salinity by farmers	Australia
[84]	Effect of salinity on eucalyptus trees	SE Australia
[85]	Soil salinity and groundwater properties	Tunisia
[86]	Extension of groundwater acidity	NSW, Australia
[87]	EM38 and TDR: comparison of measuring methods	-
[88]	Assessment of soil quality properties with EC_a	California, USA
[89]	ECa distribution in the landscape and as a consequence of evapotranspiration and phreatic rise	South Australia
[90]	Salinity in vineyards	Australia
[91]	EC_a–salinity–water content	California, USA
[92]	Salinity management in cotton fields	California, USA
	EM38 in combination with other sensors	
[93]	Comparison tools and methods detection salinity	Australia
[94]	EM38 in combination with satellite-based navigation methods	Alberta, Canada
[95]	Increasing precision of salinity with EM38 and EM31 (both EC_{ah}) at various layers	Yellow River Delta, China
[96]	Hyperspectral data related to different soil salinization extent was combined with ECa order to establish a soil salinization monitoring model	Weigan River, China

Corwin and Lesch [97] summarized five methods that have been used for determining soil salinity in the field: (1) visual crop observations; (2) the electrical conductivity of the soil solution (soil paste or extracts); (3) in situ measurement of electrical conductivity with electrical resistivity (with the Wenner array method); (4) non-invasive measurement of electrical conductivity with EC_a and, most recently; (5) in situ measurement of electrical conductivity with time domain reflectometry. Frequently, EC_e (e.g., conductivity of aqueous extracts of soil saturated soil paste, $EC_{1:5}$, $EC_{1:2}$ or $EC_{1:1}$,

conductivity of soil: water suspensions) was indicated as the most useful and reliable measurement of point-wise salinity detection [43–57,81,82,95–98]. In older publications, EC_e alone was often used to identify salt-affected areas [29–57,81,82,86,93,95–99] Norman [30] developed a salinity classification system based on the range of total dissolved salt concentration ($EC_{1:5}$) with corresponding groupings of crops with different tolerances to root zone salinity. Soil salinity can be derived from the conductivity of the bulk soil (EC_a). For example, salinity is quantified and monitored in irrigated agricultural areas of arid zones by means of EC_a measurements using EM38 [28–40,86]. In areas where saline soils exist, 65% to 70% of the variance in EC_a can be explained by the changes in salinity alone [51]. EC_a readings can be used to predict the exchangeable sodium percentage and EC_e as well [27]. The different terms of salinity can be inferred from the equation $EC_a = f(EC_{e(0-Z\,cm)})$.

During the last three decades, several calibration methods have been published describing EM38-EC_e relationships [27,28,41,60]. Following the classification of Triantafilis et al. [43] and Vlotman et al. [49], further calibration approaches have been proposed, using linear regression, multiple regression coefficients [15,31,37], simple depth weighted coefficients [5,13–55,67,69–82,86–94], established-coefficients [10,11], modelled coefficients [38], mathematical coefficients [9], a logistic profile model [43] and inverted salinity profiles [56].

Johnston et al. [19] reported that EM38 readings are not highly accurate but that categories of soil salinity for large areas can be readily established. Coefficients of determination between 0.88 and 0.9 at depth levels of 30–60, 60–90 and 0–90 cm in soils in which salinity was the dominant factor influencing the EM38 readings were described by Amezketa [59]. A more complex example of these regressions is the dual pathway parallel conductivity (DPPC) model developed by Rhoades et al. [32]. This model indicates the major contribution to EC_a readings from conductivity in the water-filled pores that contain the majority of the solved salts with a relatively small contribution from the exchangeable cations. When comparing different EC_a-EC_e prediction models, the relationships often show low accuracy [5,19,78]. These results suggest that it is essential to establish calibration relationships between EC_a and EC_e that depend on the soil type and water status for the specific site conditions for a particular survey [19,20]. The variability of EC_a to EC_e conversion is greater in coarse-textured soils than in medium- or fine-textured soils [24].

The effect of soil salinity and soil water content on the EC_a has been described e.g., by Hanson and Kaita [91], Bennett et al. [65], Gill and Yee [16], Turnham [81] and Wittler et al. [54]. The results indicated substantial changes in the EC_a readings as soil-water content changed. A linear relationship existed between soil-water content and EC_a for each level of soil salinity across the range of measured soil water contents [91]. Norman [30] stated that, for clay soils (i.e., >40% in the top 30 cm), the water content of the soil profile should be greater than 20% to allow soil salinity values to be accurately derived from the observed EC_a data. In Iranian investigations, Rahimian and Hasheminejhad [35] found that more reliable regression equations between EC_{ah} (horizontal mode) and EC_{av} (vertical mode) and soil salinity could be derived at 35% water content in comparison to 25% water content. Arndt et al. [60] cited similar values from the USDA-Soil Conservation Service. For field surveys where EC_a was closely related to salinity, Corwin and Lesch [97] used relationships between the v- and h-mode to derive new variables. The geometric mean ($sqrt(EC_{ah}*EC_{av})$) provides a measure of the cumulative EC_a through the root zone and the ratio mean (EC_{ah}/EC_{av}) characterizes the degree of leaching. A ratio greater than 1 indicates that the net flow of water and salts is upward, and a ratio less than 1 indicates a downward net flow.

Broadfoot et al. [66] and Mankin and Karthikeyan [80] described similar classifications:

- Leached soils, where salinity increases with depth, defined by $EC_{ah}/EC_{av} \leq 1.0$
- Uniform, where salinity does not change significantly with profile depth and where $1.0 < EC_{ah}/EC_{av} \leq 1.05$, and
- Inverted salinity profiles, where salinity decreases with depth and where $EC_{ah}/EC_{av} > 1.05$.

A similar representation was chosen by Spies and Woodgate [93]. Subsoil (EM31) salinity maps and root zone (EM38) maps were combined to provide an assessment of salinity hazard. The EM38 instrument had a depth range of less than 1.5 m, while the EM31 probes had a depth range of 4 to 6 m. Triantafilis et al. [42] developed a leaching fraction model in combination with EC_a based

on the amount of deep drainage and the average root zone EC_e. However, the present investigations are not limited to the creation of real-time inventories but are also of value in forecasting temporal changes in the salinity status. Lesch et al. [100] used pre- and post-EC_a surveys to quantify the degree of salt removal from a field. However, the spatial variability impeded the derivations, particularly for subareas with high salinity levels. Salama et al. [101] related apparent conductivity to recharge/discharge mechanisms within watersheds. They associated low values of EC_a with low concentrations of total soluble salts and recharge areas. Discharge areas were associated with high values of EC_a, indicating greater concentrations of soluble salts near the surface and inverted salt profiles. The latter were associated with rising groundwater tables, increased groundwater flow with mobilization of soluble salts, and greater discharge at or near the surface. All of these factors are related to saline seep development [102].

In an advanced application, EM38-EC_a was used to help to assess the salt tolerance of trees, forages and turf grasses [14,16,23–26,65]. The authors also studied the usefulness of EC_a to predict the survival and growth of eucalyptus and pastures in saline soils. According to McKenzie et al. [24,25] and McKenzie [26], close correlations between salinity measured as EC_a to the yield of wheat and salinity measured by the saturated paste extract by McKenzie [26] were equal. In contrast, relationships of EC_a with observations on the establishment and growth of perennial pasture species were weak [16]. Kaffka et al. [20] reported that, in locations where crop growth were influenced by salinity, EC_a was useful for estimating optimum N-fertilizer application and for identifying areas of the field with unprofitable yields. Horney et al. [92] developed a four-step method for site-specific salinity management in commercial fields. The steps included (1) generation of an EC_a map; (2) directed soil sampling for EC_e; (3) determination of the estimated amendment requirement as a function of location in the field; and (4) integration of the individual amendment requirements into a practical spatial pattern for amendment application. As early as 1997, McKenzie et al. noticed that EM38 is a cost-effective tool for assessing field salinity and for use in experiments on the salt tolerance of crops.

Vaughan et al. [48] combined EC_e and water content of soil samples with field wide EC_{ah} measurements. The prediction of soil salinity at unsampled points was carried out by co-kriging of $logEC_e$ with EC_{ah}. In a comparison to the work of Triantafilis et al. [44] co-kriging and regression kriging of the EC_a readings also showed minimum errors compared to ordinary and three-dimensional kriging.

All of the cited procedures are practical only if salinity is the main factor influencing EC_a and if EC_e shows a close relationship to EC_a [65]. Otherwise, a multiple regression model with further independent influencing factors is required. Consequently, calibration equations and modelled results cannot be used on other sites very often.

4. Detecting Soil-Related Properties in Non-Saline Soils by EM-38

4.1. Influence of Soil Water Content Conditions

In soils where salinity is not a significant factor, EC_a values primarily represent as a function of soil water content and the amount of electrical charge. Many researchers recommend measurements with the EM38 at a soil water content close to or at field capacity [49,103,104].

This praxis has its basis in the theory of Rhoades et al. [32] and Corwin and Lesch [97]. In sufficiently wet soils, soil water is the major conductive pathway. Here EC_a is determined by the volumetric content of soil water. However, to an increasing extent of researchers noticed that the spatial patterns of EC_a, measured under different soil water conditions, are relatively stable with time; only the level indicates a change [105]. However, the relationship between EC_a and soil physical and chemical properties varied considerably depending on the actual water conditions. This weak temporal stability of relationships between EC_a and other soil properties indicated that soil water conditions have a significant influence on EC_a. When there is not enough water in the continuous pores, the surfaces of soil particles and the small discontinuous pores of the soil are the main pathways (e.g., when soil water content is <60 to 70% of field capacity). Under these conditions, the

influence of the soil particle volume, the volume and conductivity of water in the small pores, as well as the surface- conductivity of soil particles, increases [32].

Bang [106] showed that several variables (i.e., bulk density, percentage of sand, silt, and clay, plant-available water content, cone index, and saturated hydraulic conductivity) and chemical parameters (i.e., extractable P and K, pH, cation exchange capacity, organic matter, and micronutrients) presented different strengths of the correlations with EC_a. Few direct strong correlations were found between EC_a and the soil physical properties studied ($R^2 < 0.50$), yet overall, the correlation improved when EC_a was measured under relatively dry conditions. Furthermore, according to Bang, the utility of EC_a as a variable in cluster analysis to indicate management or soil sampling zones was influenced by variations in EC_a measured under different soil water conditions. Bang suggested "that the spatial and temporal EC_a variability measured under different soil water conditions could be a critical factor when evaluating the ability of EC_a to predict soil chemical and physical characteristics important to soil and crop productivity and management". Therefore, Bang [106] recommended that an EC_a survey be conducted under relatively dry conditions in similar coastal plain soils.

Lück et al. [107] carried out measurements on loamy fields, partly with coarse textured sediments. The authors found the most pronounced EC_a distributions during summer (relatively dry conditions). This may has been caused by the larger water content fluctuations in the sandy soils due to their lower water-holding capacity. In contrast to these soils, the loamy parts of the fields had a higher water content as a consequence of higher water-holding capacity as well as better water delivery via capillary rise. Conversely, at sites with dominant Pleistocene loess soils, readings taken during periods when soil water content was at field capacity produced more pronounced maps [108]. Under drier conditions, the EC_a readings indicated lower, more similar values. Some researchers recommend a different procedure. Mertens et al. [109] suggested the creation of an averaged map from repeated recordings made at different dates. This procedure is scientifically more appropriate than a water correction. Zhu et al. [110] indicated that the best mapping of major soil distribution across a landscape studied in Pennsylvania required optimal timing, meaning the occurrence of a wet period. No single survey or relative differences in EC_a obtained by repeated measurements was sufficient to obtain the best possible soil map for the study area. A combination of repeated surveys, depth to bedrock, and terrain attributes provided the best mapping of soils in this agricultural landscape and doubled the accuracy of the map. EC_a measurements collected during the wetter periods (i.e., >10-mm antecedent precipitation during the previous 7 days) showed greater spatial variability (i.e., greater sills and shorter spatial correlation lengths), indicating the influence of soil water distribution on soil EC_a [111].

4.2. Soil Texture

Frequently, in non-saline soils, EC_a is used to indicate soil texture, particularly clay content. Simulations of silt and sand are rare and seem more likely a by-product. However, the quality of the single relationships are often rather confounding (Table 2). As noted by Corwin and Lesch [112] the target variables correlate inconsistently with EC_a mainly as a consequence of: (1) the complex interaction of soil properties; (2) a temporal component of variability that is only weakly indicated by an expected constant variable such as EC_a and (3) variable climatic factors.

McBratney et al. [113] and McBratney and Minasny [114] demonstrated that differences in the mineral composition influence the magnitude of the EC_a values and therefore the strength of the relationship to the clay content. Kaolin-dominant soil minerals will have smaller conductivities, and soil that mainly contains illite or has a mixed mineralogy will have larger EC_a values, but these values are smaller than those for smectitic materials. Furthermore, the authors noticed that at low conductivities (<50 mS m^{-1}), it is quite difficult to separate clay. Wayne et al. [115] derived texture fineness classes from EC_a readings. A conductivity greater than 30 mS m^{-1} indicated clay, and a conductivity less than 5 mS m^{-1} indicated sand. Furthermore, EC_a values between 0 and 10 were classified as sandy loam, and values between 10–20 mS m^{-1} indicated clay loam. These fineness classes represented a basis for the derivation of the plant-available water content. Domsch and Giebel [116]

described another approach to delineate clay content. Working with predominantly sandy soils, the authors indicated that, at field capacity, EC_a reflected this property well. However, for soils with water-influenced horizons (gleyic soils), such relationships are very weak and should not be introduced in calculations for mineral soils. A factor scoring that used clay and silt content showed a closer relationship with EC_a. Furthermore, the authors related EC_a to soil textural classes: an EC_a of 0–10 mS m^{-1} indicated sand or loamy sand, an EC_a of 10–20 mS m^{-1} indicated sand or loamy sand over loam, and an EC_a of 20–30 mS m^{-1} indicated sandy loam or loam. Vitharana et al. [104] used the geometric mean $((EC_{av} \cdot EC_{ah})^{0.5})$ to delineate the clay content of the top- and subsoils. Doolittle et al. [117] used EC_a to locate small inclusions of sandy soils within a predominately fine-textured alluvial landscape. Bobert et al. [103] improved the relationships between EC_a and clay, silt and clay + silt by extracting the drift caused by soil water content calculated from a wetness index map. A multi-site/multi-season approach to calibrate EC_a models for predicting clay content across large landscapes was developed by Harvey and Morgan [118]. The fact that the relationships between clay and EC_a were similar in all 12 fields, indicated that a single linear regression model could be used to describe the spatial variability of the clay content across all of the fields. This "single calibration approach" used data from a designated calibration area to estimate EC_a model parameters that were then combined with data from subsequent fields to predict the soil variability in the observed fields. The single calibration approach is likely applicable to other areas, providing requirements for its use are met. Those requirements include the following: (1) the distribution of the soil property or properties of interest in calibration area should be representative of the study area; (2) the soil property or properties that influence EC_a should be the same across the study area; and (3) management practices (e.g., crop rotation and irrigation) should be similar across the study area.

To an increasing extent, methods other than linear regression have been used. Response surface sampling design, fuzzy k-means classification, hierarchical spatial regression modelling and EC_a (EM38 and EM34) surveys were applied by Triantafilis and Lesch [119] to produce a map of spatial clay content. Triantafilis et al. [44] combined EC_a values (EM38 and EM31) and clay content with different geostatistical methods (co-kriging, regression-kriging and ordinary-kriging). The results suggested that the linear relationship of clay content against EC_a (EM38) data used in combination with kriging of regression residuals was the most accurate. Vitharana et al. [104] showed that standardized ordinary kriging of subsoil clay content as the primary variable and the geometric mean $((EC_{av} * EC_{ah})^{0.5})$ as the secondary variable gave better results when compared to ordinary kriging and traditional ordinary kriging.

Table 2. References indicating relationships between EM38-EC_a and soil texture.

Study	Texture	Texture Content (%)	EC_a (mS m^{-1})	R^2	Location of Investigations
Europe					
[103]	Clay Silt Silt + Clay	not described	EC_{av}: 10–110	0.28/0.53 * 0.14/0.49 * 0.25/0.71 * * with extracting TWI-trend	Wulfen, Kassow, East Germany
[116]	Clay Silt	4–16 7–36	EC_{av}: 3–30	EC_{av}: 0.55 (clay) EC_{av}: 0.67 (clay + silt) (after factor scoring)	Brandenburg, Berlin, Germany
[120]	Clay	2–60	EC_{av}: mean 13–92	EC_{av}: 0.56	Saxony-Anhalt, Germany
[121]	Clay	2–45	EC_{av}: 2–80	EC_a: 0.66 EC_a corr: 0.85, corrected across field boundaries with neighbors regression	Bavaria, Germany
[122]	Clay	6–42	EC_{av}, EC_{ah}: 6–36	EC_{av}: 0.08–0.38 EC_{ah}: 0.13–0.33	Scheyern, Germany

Table 2. *Cont.*

Ref.	Soil				Location
[123]	Clay	7—32	EC_{av}: 8–44 EC_{ah}: 6–41	EC_{av}: 0.21–0.44 EC_{ah}: 0.13–0.67	Scheyern, Germany
	Silt	4–53	EC_{av}: 8-44 EC_{ah}: 6–41	EC_{av}: 0.11–0.46 EC_{ah}: 0.01–0.60	
	Sand	28–79	EC_{av}: 8–44 EC_{ah}: 6–41	EC_{av}: 0.04–0.38 EC_{ah}: 0.13-0.69	
[109]	Clay Silt Sand	2–25 5–69 5–50	EC_{av}: 5–65	EC_{av}: 0.76–0.76 EC_{av}: 0.65–0.71 EC_{av}: 0.00–0.69	3 fields around Bonn, Germany
[108]	Clay	3–48	EC_{av}: 2–99 EC_{ah}: 5–77	EC_{av}: 0.76 EC_{ah}: 0.74	South Germany
	Silt	4–71	EC_{av}: 2–99 EC_{ah}: 5–77	EC_{av}: 0.67 EC_{ah}: 0.67	
	Sand + gravel	15–67	EC_{av}: 2–99 EC_{ah}: 5–77	EC_{av}: 0.76 EC_{ah}: 0.74	
[124]	Clay	5–30	EC_{av}: 9 (mean)	EC_{av}: 0.94	Southwest Sweden
[125]	Clay	9–24	EC_{av}: 4 EC_{ah}: 32.2 approximate values two depths: 0–25 cm, 25–60 cm and 2 fields	EC_{av}: 0.19–0.41 EC_{ah}: 0.32–0.45	South Norway
	Silt	28–49		EC_{av}: 0.006–0.52 EC_{ah}: 0.002–0.56	
	Sand	33–61		EC_{av}: 0.01–0.4 EC_{ah}: 0.02–0.44	
	Gravel	3–11		EC_{av}: 0.05–0.94 EC_{ah}: 0.08–0.94	
[126]	Clay	about 5–40	EC_{ah}: 6–26	EC_{ah}: 0.63	South Norway
[127]	Clay Sand	23–44 39–67	EC_{av}: 0–50	EC_{av}: 0.55 EC_{av}: 0.41	Moravia, Czech Republic
[128]	Clay	4–24		EC_{av}: 0.49–0.67 (different dates on the same field)	Jütland, Denmark
[129]	Clay	2–56	EC_{av}: 9–106 EC_{ah}: 5–97	EC_{av}: 0.81	East-Flanders, Belgium
[104]	Clay	topsoil: 14–24 subsoil: 3–27	EC_{av}: 18–47 EC_{av}: 12–36	$(EC_{av}{}^{*} EC_{ah})^{0.5}$: 0.69 subsoil $(EC_{av}{}^{*} EC_{ah})^{0.5}$: 0.16 topsoil	Flanders, Belgium
North America					
[106]	Clay	10–46 (mean values)	EC_{av}: 1–54 EC_{ah}: 1–56	EC_{av}–30 cm: about 0.5 EC_{ah}–30 cm: 0.3–0.56	North Carolina, USA
	Silt	20–35 (mean values)	EC_{av}: 1–54 EC_{ah}: 1–56	EC_{av}–30 cm: 0.4–0.6 EC_{ah}–30 cm: −0.3–0.56	
	Sand	40–70 (mean values)	EC_{av}: 1–54 EC_{ah}: 1–56	EC_{av}–30 cm: about 0.4 EC_{ah}–30 cm: −0.3–−0.6	
[130]	Clay Silt Sand	24–44 26–51 8–50	EC_{av} , EC_{ah}: about 40, salinity affected	0.08 0.18 0.14 ln of geometric mean of EC_{av} and EC_{ah}	California, USA
[112]	Clay	3–48	about EC_{av}, EC_{ah} 10-65	EC_{av}: 0.11. EC_{ah}: 0.08	Western California, USA
[131]	Clay	14–29	EC_{av}: 19–35 EC_{ah}: 14–26	EC_{av}: 0.69 EC_{ah}: 0.66	Nebraska, USA
[118]	Clay	12–32	EC_{av}: 19–118	0.76	12 sites in Texas, USA

Table 2. *Cont.*

[132]	Clay	13–63	EC_{av}: 30–65 EC_{ah}: 38–83	EC_{av}–30 cm: 0.55 EC_{ah}–30 cm: 0.55	Central Missouri, USA
	Silt	33–81	EC_{av}: 30–65 EC_{ah}: 38–83	EC_{av}–30 cm: 0.55 EC_{ah}–30 cm: 0.55	
	Sand	6–11	EC_{av}: 30–65 EC_{ah}: 38–83	EC_{av}–30 cm: 0.27 EC_{ah}–30 cm: 0.27	
[3]	Clay Silt	13–36 31–67	EC_{av}: 7–37	EC_{av}: 0.55 EC_{av}: 0.15 and 0.48 (2 fields)	North-central states, USA
[133]	Clay Silt Sand	about 5–40 unknown unknown	EC_{av}:about 5–60	EC_{av}: 0.36–0.77 EC_{av}: 0.27–0.71 EC_{av}: 0.21–0.36	Midwest USA
[100]	Clay Sand	10–32 52–85	EC_{av}: 84.8 EC_{ah}: 40.1	EC_{ah}: 0.76 EC_{ah}: 0.74	Southwest USA
Australasia					
[42,45]	Clay	about 30–85	EC_{av}:80–200 (salt affected)	EC_{av} 0.62 and 0.64	NSW, Australia
[134]	Clay	about 40–65	EC_{av}:30–210	EC_{av}: 0.72	NSW, Australia
[119]	Clay	15–58	EC_{av}: 5–159 EC_{ah}: 13–147	EC_{av}: 0.66 EC_{ah}: 0.67 combination of EM34 and EM38 in different modes:0.79	NSW, Australia
[135]	Clay	about 20–45	about 10–36	EC_{av}: 0.72 EC_{ah}: 0.65	Manavata, New Zealand
Asia					
[136]	Clay Silt Sand	1.5–41.3 6.5–33.5 45.8–91.0	EC_{av}: 1–40	topsoil: 0.47 (on average)	Sri Lanka
Unknown					
[137]	Clay	12–20	EC_{av}: 7–20 EC_{ah}: 7–15	EC_{av}: 0.78 EC_{ah}: 0.80	Not described

4.3. Soil Water Content, Water Balance

The derivation of the water storage capacity, particularly the field capacity, and the plant-available water content based on electrical conductivity measurements has gained increasing importance. Table 3 provides an overview of current investigation areas and target variables.

Table 3. Literature describing relationships between EM38-EC$_a$ and parameters of soil water.

Study	Parameters	Location of Investigations
	Water content	
[138]	Water content	Iowa, USA
[139]	Water content	Iowa, USA
[112]	Water content	South California, USA
[91]	Water content	California, USA
[140]	Water content, water table depth	New Zealand
[141,142]	Water content	Ontario, Canada
[143]	Water storage [mm]	Minnesota, USA
[144]	Soil drainage classes	Illinois, USA
[145]	Soil water content (θ_v, θ_w), ±3%	South Dakota, USA
[146]	Plant available water content	Missouri, USA

Table 3. *Cont.*

[147]	Water content	Columbia County, USA
[148,149]	Volumetric water content	Texas, USA
[122]	Water content: EC_{av}: 0.39; EC_{ah}: 0.26 Plant available water content: EC_{av}: 0.31; EC_{ah}: 0.29	Bavaria, Germany
[123]	Water content EC_{av}: 0.04–0.26; EC_{ah}: 0.16–0.64	Bavaria, Germany
[150]	Water content	Florida, USA
[3]	Water content	North-central USA
[151]	Water content with EM38 and ASD spectrometer	Quebec, Canada
[102]	Repeated EC_a measurements for determining water content	Pennsylvania, USA
[152]	Detection of available water content from EC_a, for using in the yield software ADSIM	WA, Australia
[153]	Repeated EC_a measurements and relation to water content (irrigation)	Queensland, Australia
[115]	Available water content and soil water deficit from texture finess classes and EC_a	Cambridgeshire, UK
[154]	EC_a in combination with GPR to predict field wide water content	South-east Italy
[155]	Soil water content, soil bulk density	South Dakota, USA
Groundwater, water table depth, water drainage		
[156]	Water table depth using geophysical and relief variables	Darling River, Australia
[9]	Groundwater recharge	South Australia
[157]	Depth to groundwater table	Montana, USA
[158]	Soil drainage classes	Iowa, USA
[159]	Characterizing of water and solute distributions in the vadose zone with readings of EM38 and borehole conductivity meter	New Mexico, USA
[160]	Water table depth	Florida, USA
[161,162]	Detection of areas with different water movements	Tennessee, USA
[46]	Deep drainage risk	Australia
[163]	Hydraulic conductivity of palaeochannel in alluvial plains	NSW, Australia
[42,45]	Deep drainage (mm/year) with a 4-parameter broken-stick model fitted to EC_{av} beyond 120 cm	Australia
Irrigation		
[164]	Irrigation effectiveness/drainage	California, US,
[165]	EC_a – soil available water holding capacity on two variable-rate irrigation scenarios	New Zealand
[166]	EC_a for quick assessment of deep drainage under irrigated conditions in the field.	Australia

Water content, like salinity, is a horizontally and vertically effective dynamic property. In areas where water content is the dominant factor that influences EC_a and where water content decreases with depth, $EC_{ah} > EC_{av}$ and vice versa [167]. Wayne et al. [115] developed a hierarchical procedure for calculating available water content. EC_a was used to target the location for neutron probe samples. The construction of a water content–texture relationship allowed the determination of the available water content and the soil water deficit. Kachanoski et al. [141] found that in soils with a low electrolyte content and a wide range of texture, EC_a explained more than 90% of the water content. Additionally, Kachanoski et al. [142] correlated EC_a readings with water storage and found that 50–60% of the variations in EC_a were explained by water content. Similar levels for coefficients of determination were described by Sheets and Hendrickx [150] and Khakural et al. [143]. Morgan et al. [147] noted that EC_a is only applicable in areas with a greater range of water content. The same observation was made by Hedley et al. [135],who calculated an R^2 of 42%. Substantial changes in the relationships between EC_a readings and soil water content were shown by Hanson and Kaita [91]. The higher the soil salinity was, the more sensitive the EC_a readings were to changes

in soil water content. A linear relationship existed between soil water content and EC_a for each level of soil salinity over the range of measured soil water contents. In a Mollic catena, Brevik et al. [139] found significant relationships between EC_a and soil water content that explained 50% to over 70% of the variability. The greatest difference between EC_a values in any soils was observed when the soils were moist. Regression line slopes tended to be lower in higher landscape positions indicating greater EC_a changes with a given change in soil water content. A relationship between increasing water content and EC_a readings from a summit-to-foot slope area of calcareous till parent material with a coefficient of determination of 0.86 was described by Clay et al. Wilson et al. [161,162] derived areas with different water movements from EM31 and EM38 readings. Drying/draining patterns were characterised by a downward shift in EC_a with time. Follow-up EC_a surveys across high-to-low patterns showed a positive correlation between EC_a and water content. Regions with increased horizontal flow showed high conductivities after rainfall. Areas that had preferential vertical flow showed lower EM38 readings after periods of rainfall. For a prototype engineered barrier soil profile designed for waste containment, Reedy and Scanlon [148] and Reedy [149] predicted the average volumetric water content at any location at any time with a linear regression model ($R^2 = 0.80$) and spatially averaged volumetric water contents over the entire area ($R^2 = 0.99$).

Bang [106] described weak and negative relationships between soil water content and EC_a values in North Carolina's Coastal Plains. Little variation in subsoil water content across the study site for each survey date combined with a relatively narrow range of variability in soil texture was the main reason for this result. Furthermore, the variability in other factors (e.g., soil compaction and texture) might have masked the contribution of the water content to EC_a variation., The author concluded that the spatial variability of soil water content at a 0- to 75-cm depth could not be directly determined by a field-scale EC_a survey at this site, due to the weak relationships between soil water content and EC_a. Relationships between plant-available water content and EC_a ($R^2 = 0.78$) were derived by Wong and Asseng [152] to transform a water storage capacity map of the field into yield maps for three major season types (dry, medium and wet) and nitrogen fertilizer management scenarios. Hall et al. [159] reported that EC_a methods (i.e., EM38 and the use of a borehole conductivity meter) could accurately characterize water and solute distributions in the vadose zone. Saey et al. [168] developed an index to register the area-wide soil heterogeneity. After calculating the relationship between clay content and EC_a, this equation was converted so that EC_a was the target variable. In the next step, the authors calculated a quotient of the measured EC_a and the EC_a reading derived from the clay content. This result was called EC_{ref} and was used as measure for soil heterogeneity.

Variables other than water content are targets of EC_a measurements to an increasing extent; for example, hydraulic conductivity, water table depth, drainage classes and groundwater recharge. In developing a relationship between EC_a and estimated deep drainage (mm/year) Triantafilis et al. [42,45] developed four-parameter broken-stick models fitted to EC_{av} beyond 120 cm. Vervoort and Annen [163] showed that the overall patterns of the hydraulic conductivity of palaeochannel in alluvial plains could be inferred from the combination of EM inversion using EM38 and EM34 measurements. However, the absolute magnitude of hydraulic conductivity could not be easily predicted.

Sherlock and McDonnell [169] used simple linear regression analyses to compare terrain electrical conductivity measurements from EM31 and EM38 to a distributed grid of water table depth and soil- water content measurements in a highly instrumented 50 by 50 m hill slope in Putnam County, New York. Regression analysis indicated that EC measurements from the EM31 meter (v-mode) explained over 80% of the variation in the water table depth across the test hill slope. Despite problems with sensitivity and zeroing the EM38 could explain over 70% of the gravimetrically determined soil water variance.

The depth of the water table was also detected by Schuman and Zaman [160]. Knowledge of the water table depth was necessary to select a suitable field for new citrus plantings and for drainage systems. With EC_a in the vertical mode, the authors could estimate these values with a RMSE of approximately 4–15 cm. EC_a, the topographical wetness index and the rainfall time series gave good predictions of water content and water table depth using the models derived according to Hedley et

al. [140]. Further investigations determined soil drainage classes [144], groundwater recharge [170], water drainage [46] and irrigation [164].

4.4. Detection of Soil Horizons and Vertical Discontinuities

To an increasing extent, investigations were carried out to calculate EC_a depth profiles in combination with the detection of vertical discontinuities (Table 4). Refining and improving of soil maps is necessary for soil protection and the description of soil functions.

Table 4. Literature indicating derivations of soil types and patterns as well as further soil parameters from EM38-EC_a.

Study	Investigation Object	Location of Investigation
	Soil types	
[171]	Separation between Natraqualf and Ochraqualf	Tennessee, USA
[172]	Soil types, yield maps	Virginia, USA
[173]	EC_a to derive more homogeneous lacustrine-derived soils	Iowa, USA
[174]	Soil pattern as basis of management zones	England
[175]	Soil boundaries	Denmark
[158]	Soil map unit boundaries, detection of inclusions	Iowa, USA
[2]	Refine and improvement of soil maps	-
[176]	Soil types with clusteranalysis	Elbe-Weser-region, Germany
[177]	Detection of areas with sulfidic sediments and coastal acid sulfate soils	NSW, Australia
[128]	Soil types	Jütland, Denmark
[178]	Soil boundaries between clay loam and sandy loam soils	Cambridge, UK
[179]	Soil types, in combination with terrain parameters and other sensors	NW Victoria, Australia
[102]	Repeated EC_a measurements for determining soil types	Pennsylvania, USA
[180]	Inversion of EM38 and EM34 sigma-a data to detect the areal distribution of soil types	Darling River, Australia
[181]	Distinguishing between soils with cambic pedogenic horizons and argillic horizons; boundaries of soil map units	Texas, USA
[182]	Supporting delineation of spatial distribution of C content	Harz region, Germany
	Soil depth to horizons/layers/discontinuities/borders	
[183]	Depth to limestone bedrock and clayey residuum	Florida, Pennsylvania, USA
[184]	Depth of claypan soils	Missouri, USA
[185]	Soil depth sounding	East, south Germany
[5]	Soil depth sounding	Ontario, Canada
[186]	Depth to sand and gravel	Unknown
[187]	Depth of sand deposition	Missouri, USA
[188]	Layer depth, EC_a as auxiliary variable	North Netherlands
[189]	Depth of the Tertiary substratum	Flanders, Belgium
[190]	Soil depth to petrocalcic horizon	Utah, USA
[191]	Soil depth to bedrock (loess above basalt)	Idaho, USA
[192]	Bulk density and EC_a	Iowa, USA
[193]	Boulder clay depth	North Netherlands
[194]	Linear, negative relation between EC_a and topsoil layer thickness	Fuxin, China
[195]	Bayesian method to map the clay content of the B_t horizon associated with the control of encroaching trees	South Africa
[1,196–198]	Depth to claypan soils	Missouri, USA

Table 4. *Cont.*

	Further soil properties	
[88]	Soil properties and cotton yield	California, USA
[199]	Soil properties and cotton yield	California, USA
[112]	Water content, cation exchange capacity, cations and anions in saturation extract and exchangeable, B, Mo, pH, C, N,	West California, USA
[132]	Cation exchange capacity, C, N, P, soil enzyme, microbial biomass, hydr. Sat. K., bulk density	Missouri, USA
[3]	Water content, cation exchange capacity	North-central states, USA
[45]	CEC in salt affected soils	NSW, Australia
[200]	CEC in dependence of EM38, EM31, 3 remotely sensed (Red, Green and Blue spectral brightness), 2 trend surface (Easting and Northing) variables	NSW, Australia
[201]	Exchangeable Ca, Mg, cation exchange capacity	Ontario, Canada
[124]	EC_a as a covariable in cokriging improved the prediction of pH, clay, SOM	Sweden
[202]	EC_a in relation to water content, yield, CEC, clay silt, organic matter	Brandenburg, Saxony-Anhalt, Germany
[131]	C, total dissolved solids, depth of topsoil	Nebraska, USA
[203]	Soil organic carbon and classifing with fields normalized EC_a	Andalucia, Spain
[204]	N-dymanics for management zones	Nebraska, USA
[176]	Precision agriculture: combination of EC_a and soil parameters (clay, yield, plant available water)	Mecklenburg, Germany
[205,206]	Compaction in paddy rice fields by puddling	Bangladesh
[207]	EC_a as subsidiary variable for interpolation	Missouri, USA
[208]	Soil compaction	Silsoe, UK
[209]	Relations leaching rates to EC_a	NSW, Australia
[210]	EC_a as subsidiary variable for interpolation of P, K, pH, organic matter and water content	Iowa, USA
[211]	Simple linear inversion of EC_a to simulate magnetic susceptibility	-

EC_a profiling by depth requires more intensive measurements. Usually, this investigation is carried out with measurements made at different heights above the soil surface or repeated measurements at different coil spacing using regressions between EC_a and depth for the further calculation [5,9,185,212]. As the instrument is raised above the ground, the relative influence of deeper layers on the measurements decreases. Visual comparison of EC_a values and instrument height and inverse modelling (inversion, optimization) are often used. However in numerous cases, the alternating influencing factors impede the retrieval of adequate results; for example, both texture and salinity can cause strong vertical fluctuations. Sudduth et al. [196], Sudduth and Kitchen [155,175–179,181,184–188,195–198,201–209], Kitchen et al. [213] and Noellsch [214] used EC_a to determine the depth to the claypan (the sublayer with 50 to 60% clay, varying in depth from 0.1 to 1 m) in nonsaline soils (Missouri). A high correlation between increasing EC_a and decreasing depth to the claypan was observed by Doolittle et al. [184]. The depth of boulder clay was estimated by Brus et al. [193], and Bork et al. [191] estimated the loess thickness above basalt. Mapping of sand deposition after floods was carried out by Kitchen et al. [187]. In the investigations of Boettinger et al. [190] soil depth to the petrocalcic horizon was positively and significantly correlated with EC_a. Doolittle and Collins [183] reported that bedrock depths on a Pennsylvania site, based on depth classes, could be estimated with EC_a data.

Knotters et al. [188] introduced EC_a as an auxiliary variable in co-kriging and kriging with regression to predict the depth of Holocene deposits. Vitharana et al. [189] improved the content of a soil map with the calculation of the depth of a Tertiary stratum.

4.5. Relationships to N-turnover, Cation Exchange Capacity, Organic Matter and Additional Soil Parameters

In addition to the previously listed soil properties, further parameters have been combined with EC_a readings, including cation exchange capacity, organic matter, bulk density, nutrients (e.g., NO_3^-, Olsen-P) and elements such as Ca, Mg, K, Na (exchangeable or in saturation extract), B, Mo, H and other anions. For close relationships, field-wide ECa measurements allow mapping of soil properties (Table 4). The dominant target variable was the cation exchange capacity [3,132,135].

The leaching rates calculated from a field study were related to changes in EC_a readings [209]. This enabled the derivation of a spatially averaged leaching rate. The spatial distribution of N seems to be an increasingly attractive parameter to be estimated via soil conductivity. Eigenberg and Nienaber [215,216] and Eigenberg et al. [217,218] related EC_a maps made at different times to temporal values of available N and other specific mobile ions that were associated with animal waste and cover crops, and concluded that EC_a can be used as an indicator of the content and loss of water-soluble N. Eigenberg and Nienaber [215,219] isolated and detected areas of nutrient build-up in a cornfield receiving waste. Different manure and compost rates had been applied for replacement of commercial fertilizer. EC_a measurements differentiated commercial N-fertilized plots from those that had manure applied at the recommended P rate, compost applied at the P rate, and compost applied at the N rate. In another publication, the same authors [220] discriminated areas with synthetic fertilizer from areas with feedlot manure and compost application. Differences between EC_a maps before and after the applications were partly explained by N decompositions. Furthermore, Eigenberg et al. [221] reported that EC_a (EM38 and Dualem-2) soil conductivity appeared to be a reliable indicator of soluble N gains and losses in a soil under study in Nebraska, a measure of available N sufficiency for corn mainly in the early growing season, and an indicator of NO_3^--N surplus after harvest when soluble N was vulnerable to loss as a consequence of leaching and/or runoff.

Johnson et al. [204] stated that in soils where EC_a is dominated by NO_3^--N, EC_a was applicable for tracking spatial and temporal variations in crop-available N (manure, compost, commercial fertilizer, and cover crop treatments). Furthermore, the calculation of fertilizer rates for site-specific management was possible. Stevens et al. [222] studied EC_a as an indirect measure for NH_4^+ and K^+ in animal slurries. The predictive capability of soil conductivity to estimate soil nitrate was demonstrated by Doran and Parkin [223]. Korsaeth [125] found an explanation of a variance of 27–69% (average 47%) of topsoil inorganic N concentration by means of EC_a. In general, the author stated that determination of absolute levels of this parameter was difficult with EC_a, but it appeared to be quite a robust method for detection of both spatial and temporal relative differences. Some authors described relationships between ECa and soil conditions that influenced soil mineral N [224,225]. Fritz et al. [224] suggested the application of ECa to predict NO_3^- concentrations in the soil. A comparison of the EM38 and the Veris 3100 sensor cart showed a correlation with soil NO_3^-, but the authors indicated that further studies were necessary to confirm their results.

The studies of Jaynes et al. [226] and Kitchen et al. [213] assumed a possible relationship between soil ECa and N mineralization and denitrification rates. Soil conditions, especially the texture, influenced the rate of denitrification and N mineralization [227]. The relationships between soil texture and N mineralization and denitrification should aid in developing an in-season variable-rate N fertilizer recommendation [224]. Soil organic matter, ECa, and soil texture are properties that might aid in predicting mineralization and denitrification in soil. Dunn and Beecher [228] detected large differences in surface soil acidity and a strong relationship ($R^2 = 0.49$ to 0.91) compared to EC_a readings in individual rice fields in NSW, Australia. The proposed EC_a levels for the delineation of zones were <80, 80–140 and >140 mS m^{-1} for the EM31 vertical mode, and <80, 80–110 and >110 mS m^{-1} for the EM38 vertical mode. Many rice growers in southern NSW currently have EM maps of their fields. Using these maps soil sampling for soil acidity would be a more cost-effective method than grid sampling.

Triantafilis and Momteiro Santos [200] indicated the cation exchange capacity (CEC) as one of the most important soil properties because it is an index of the shrink–swell potential and is thus a measure of soil structural resilience to tillage. The authors used the readings from EM38 and EM31,

and additionally remotely sensed spectral reflections (red, green and blue spectral brightness), and two trend surface (Easting and Northing) variables as ancillary data or independent variables, and a stepwise MLR model was used to predict the CEC. The x and y variables accounted for any distinct drift in the residual error pattern. The correlation coefficient ($R^2 = 0.76$) for the regression model was much larger than that achieved with any of the individual ancillary data variables. The adjusted R^2 was 0.69, and the estimated RMSE was 1.86 cmol kg^{-1}.

In other studies, the results were more confusing. Heininger et al. [229] and Nadler [230] indicated that salinity, soil texture, or soil water content were masking the response of EC$_a$ to other physical, chemical and nutrient levels in soil. Cations, such as Ca, Mg, or K, commonly associated with binding sites on soil particles, could influence EC$_a$ with variations in EC$_S$ (i.e., conductivity of the solid soil). However, the common assumption is that in most field solutions, changing levels of soil cations have a minor influence on EC$_S$ [229,231]. Heininger and Crosier [232] demonstrated that under saturated conditions changes in nutrient levels (e.g., soluble N and S), changes in EC$_{wc}$ could influence EC$_a$. In a study by Heiniger et al. [229], EC$_a$ was evaluated as a means to estimate plant nutrient concentrations (i.e., P, K, Ca, Mg, Mn, pH, CEC, and humic content). This study indicated that it was unlikely that ECa could be used to directly estimate the soil nutrient content in a field. However, the authors suggested that additional research on the relationships of EC$_a$ with soil water content and soil texture was necessary to determine whether EC$_a$ could be used to establish nutrient management zones. The authors concluded that "EC$_a$ can be valuable tool when used in conjunction with multivariate statistical procedures in identifying soil properties and their relationship to nutrient availability".

According to Martinez et al. [203], EC$_a$ can provide inexpensive and useful information to capture soil spatial variability and characterization of organic carbon. EC$_a$ data were used to elucidate differences in soil properties as a consequence of topography and management, explaining >25% of the spatial variation. With normalized EC$_a$ (ΔEC$_a$) the authors successfully applied fuzzy k-means to delimit homogeneous soil units related to soil management and the spatial distribution of organic carbon. Grigera et al. [131] related soil microbial biomass to organic matter fractions in a field using EC$_a$. Soil properties (0–90 cm) that showed higher correlations with EC$_{av}$ (C$_t$ ($R = 0.87$), clay ($R = 0.83$), total dissolved solids ($R = 0.68$), and depth of topsoil ($R = 0.70$)) influenced soil water availability in this field. Soil microbial groups were correlated with different soil C fractions in the uper 15 cm and were similar across EC$_a$ zones. Motavalli et al. [233] assessed variation in soil Bray 1 P levels in litter amended landscapes at 0–5 and 5–15 cm depths. EC$_a$ was also applied as subsidiary variable in a co-kriging method for improving the map accuracy interpolation of P, K, pH, organic matter and water content [210]. Jung et al. [207] described a similar effect for the application of EC$_a$. Cross-semivariance analysis with EC$_a$ as a secondary variable were better than by a simple semivariance analysis.

Bekele et al. [234] reported that EC$_a$ was strongly related to ammonium extractable K, organic matter (OM), pH and Bray-2 phosphorus with factor analysis but not to ammonium extractable Ca and the sum of bases in fields in LA, USA. Furthermore Lukas et al. [127] examined soil chemical characteristics (i.e., P, K, Mg content and pH value) and humus content and showed relatively balanced, moderately strong correlations with EC$_a$.

Additionally, the use of EC$_a$ for the detection of soil compaction has become increasingly important [192,208]. Krajco [208] discovered that the EC$_a$ readings measured in the horizontal mode distinguished the areas with no compaction above 0.3 m and areas with soil compacted in the entire soil profile with less precision. The EM38 operated in the vertical mode was not sensitive enough to measure any differences in soil bulk density.

4.6. Derivation of Soil Sampling Designs

EC$_a$ measurements are frequently applied to devise soil sampling schemes to reduce soil sampling points (Table 5) [88,114,115,235,236].

Table 5. Literature describing selection of areas for soil sampling with EM38-EC$_a$.

Study	Investigation Object	Location of Investigation
[59]	Soil sampling points	Ebro River, Spain
[199]	Sampling design	West California, USA
[237]	EC$_a$ base sampling design: response surface sampling design (RSSD), stratified random sampling design (SRSD)	California, USA
[228]	Soil sampling design pH	NSW, Australi,
[238]	Mapping sodium affected soils	Great Plains, USA
[204,239]	Soil sampling design, soil units	West California, USA
[100,236, 240,241]	Soil sampling design	Southwest USA
[115]	Sampling design for loacation of neutron probe access tubes	Cambridgeshire, UK
[242]	VQT method (variance quad-tree) in combination of relief data and EC$_a$	Jiangsu Province, China,
[235]	Optimum locations for soil investigations	Brandenburg, Germany

In addition to finding representative locations, the goal is to significantly reduce the number of samples required to effectively calculate the target variable. Frequent selection of sampling points by means of EC$_a$ surveys is performed empirically. In principle, design-based (probability-based) and model-based (prediction-based) sampling schemes are applicable.

Triantafilis et al. [42,45] used the ratio (EC$_{av}$(EM38)/EC$_{av}$(EM31)) to determine soil sampling points on salt affected areas. Lower ratios appeared when EM38 was sensing the relatively sandy and less conductive topsoil. The results of Shaner et al. [243] support the utilization of EC$_a$-directed zone sampling as an alternative to grid sampling if the transition zones of soil texture and soil organic matter are avoided. Approximately 80% of the samples in grid sites 10 m from the zone boundaries were classified correctly compared to the samples <10 m from the boundary, in which only 50–54% were classified correctly. Corwin et al. [237] described a procedure that was the basis for the development of the ESAP software package [240,241]. In this model-based sampling approach, a minimum set of calibration samples was selected based on the measured ranges and spatial locations of the EC$_a$ readings. This sampling approach originated from the response surface sampling design (RSSD) methodology of Box and Draper [244]. The ESAP software was specifically designed for use with ground-based EM signal readings. The ESAP software package tried to identify the optimal locations for soil sampling (6–20 sites depending on the level of variability of EC$_a$) by minimizing the mean square deviation. Zimmermann et al. [235] developed a hierarchical system with (1) EC$_a$ measurements; (2) kriging; (3) cluster analysis; (4) principal component analysis and (5) formation of a pseudo-response surface design to select subsets of appropriate sites for soil sampling. The number of samples could be minimized while still retaining the prediction accuracy inherent in statistical sampling techniques. Horney et al. [92] suggested a methodology for salt affected soils with the following steps: (1) building an EC$_a$ map; (2) directed sampling for salinity; (3) as a function in the field determination of the estimated improvement requirement and (4) integration into a practical spatial pattern. Tarr et al. [245] used stratification of EC$_a$ and terrain attributes to derive a heterogeneous pasture in relatively homogenous sampling zones with fuzzy k-means clustering. The five zones had significant differences in the target variables (i.e., P, K, pH, organic matter and water content). However, the reduction of sampling points from 116 to 30 to 15 points resulted in a loss of accuracy, but this loss may not have an economic or management consequence to the producer. Yao et al. [242] described a completely new method based on Minasny and McBratney [246]. The authors developed the application of the VQT (variance quad-tree) method on sampling design with the digital elevation model and its derivatives and Landsat TM images. EC$_a$ was selected as an additional variable, and the spatial distribution map of EC$_a$ was used as design detecting salinity. The results show that the spatial distribution of soil salinity detected with the VQT scheme was similar to that produced with grid sampling, while the sample quantity was reduced to approximately one-half. The spatial precision of the VQT scheme was considerably higher than that of the traditional grid method with respect to the same sample number. Fewer samples were required for the VQT scheme

to obtain the same precision level. The authors suggested that VQT and EC$_a$ provide an efficient tool for lowering sampling costs and improving sampling efficiency in the coastal saline region.

4.7. Derivation of Soil Type Boundaries

Delineating soil classifications has quite different levels of complexity and accuracy. ECa is applied to support the derivation of soil types (Table 4). Very often, the first question concerns the interpolation of the EC$_a$ procedure. Niedźwiecki et al. [247] gave an overview of EC$_a$ field-wide variability with variograms. The authors recommended an individual interpolation because of differing variability between fields. Selection of parameters for semivariograms has a strong influence on the ability to identify significant spatial autocorrelation of data. Lag parameter size and directional analysis of variance are particular concerns.

The next question concerns the interpolation of EC$_a$ across field boundaries. As a consequence of land use, time of measurement, wetness, and fertilization differences between single fields, considerable differences in the EC$_a$ levels frequently exist. Weller et al. [121] presented a method for unifying EC$_a$ across boundaries with a "nearest-neighbours EC$_a$ correction". EC$_a$ measurements near field boundaries were correlated with EC$_a$ values of the neighbouring field, resulting in the same level of EC$_a$ in both fields. This procedure also enhanced the coefficients of determination.

Another procedure was described by Heil and Schmidhalter [108] (Figure 3). To reduce the levels and to obtain reliable EC$_a$ values across field boundaries, the following steps were used: (1) The field-by-field means (m$_{field}$) were subtracted from individual observations (Figure 3b); (2) The resulting new EC$_a$ (z$_{residual}$) values were then used as input to estimate the residual variogram. The EC$_a$ data were interpolated, and continuous maps of EC$_a$ residuals were obtained (Figure 3c); (3) Finally, the field-by-field means (m$_{field}$) were added back to the estimated point-kriged surfaces (z$_{krig}$) for each particular field (Figure 3d). With this procedure it is possible to interpolate point wise or row wise measurements with a single interpolation calculation.
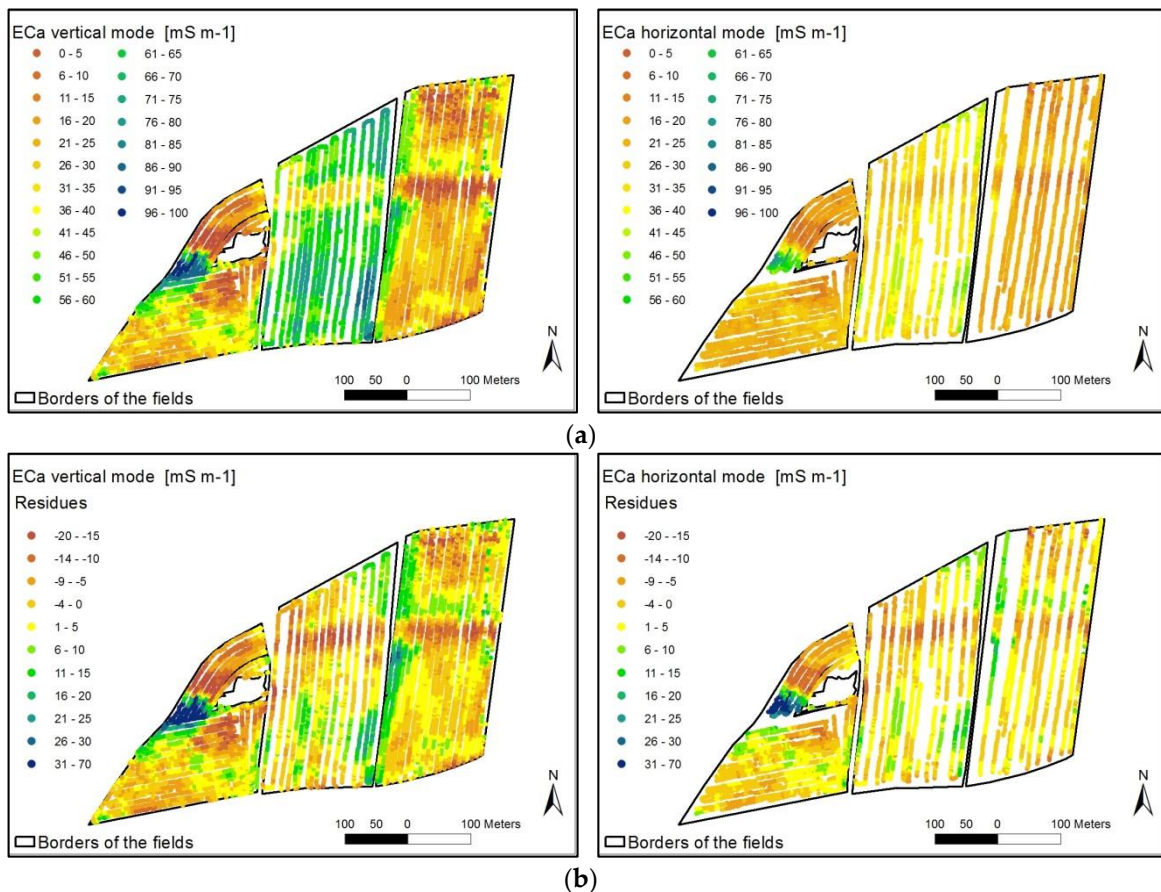

(**a**)

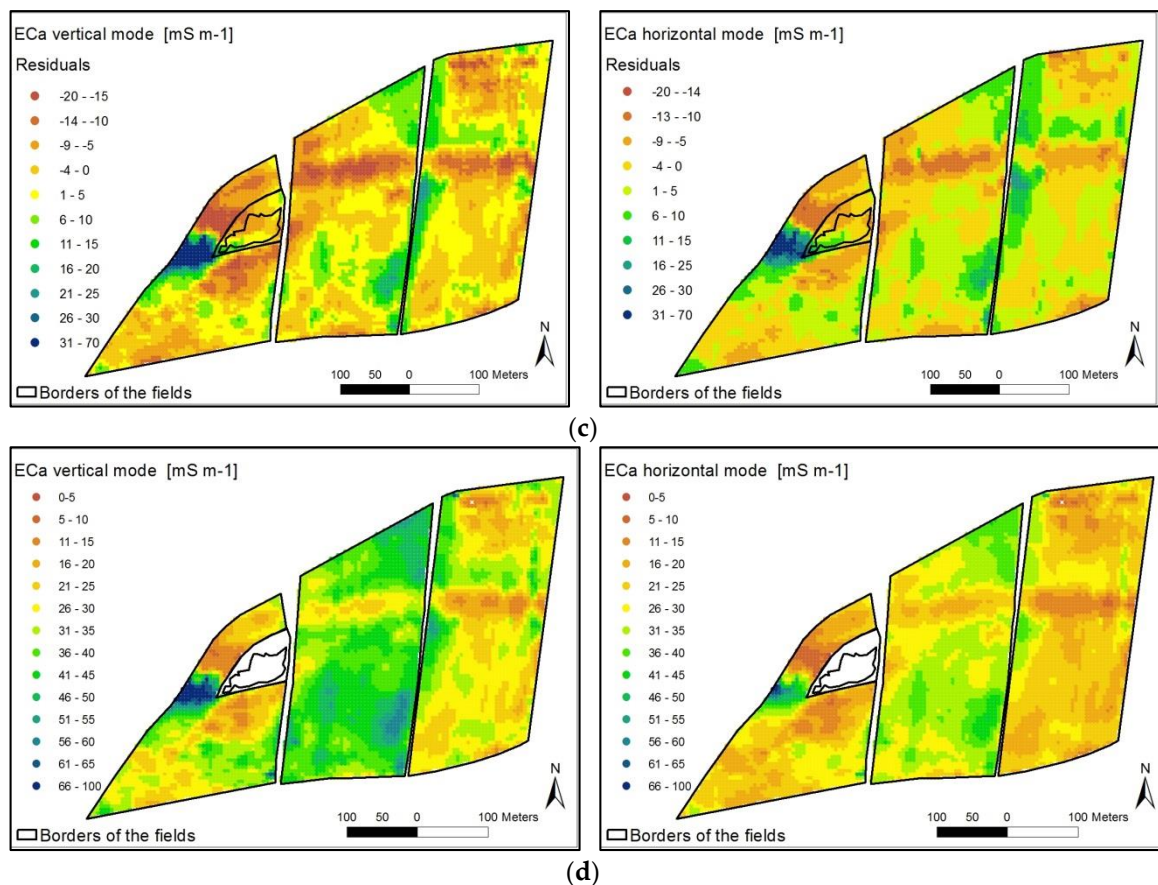(**b**)

(c)

(d)

Figure 3. Procedure of interpolation of EC$_a$ across field boundaries. (**a**) Lanes of EC$_a$ –measurements with EM38 on arable farmland (16.9 ha); (**b**) Lanes of EC$_a$ –measurements (field-by-field means (m$_{field}$) were subtracted from individual observations); (**c**) Interpolation 5 m × 5 m grid of EC$_a$ (residuals); (**d**) Interpolation 5 m × 5 m grid of EC$_a$ (residuals+local means)

Nehmdahl and Greve [128] compared soil profile descriptions and interpolated EC$_a$ measurements to derive areas with more or less similar soil types. Stroh et al. [181] distinguished boundaries of soil map units in a relative manner. In different instances, gradients or contrasting inclusions within map units were also identified. In this investigation, correlations between EC$_a$ readings and soil properties such as CEC, pH, particle size distribution and extractable bases were low (i.e., explained <6% of the variance) or non-significant. James et al. [178] used confusion matrix analysis to determine whether EC$_a$ and a clustered k-means algorithm accurately delineated soil textural boundaries in a field containing clay loam and sandy loam soils. The agreement between the EC$_a$ data and the two soil classes was 62%. Hedley et al. [135] derived two soil units (clayey soils and silty loamy soils) with a discriminant analysis of an EC$_a$ survey. A more detailed prediction was not possible.

Often, the use of EC$_a$ is restricted to its application as covariate or the readings are used in a relative sense, not as absolute terms. In some studies, combination with further predictors such as terrain attributes or yield deliver an acceptable result [179]. Rampant and Abuzar [179] predicted soil types from the various combinations of geophysical (EM38, EM31, airborne gamma radiometrics) and terrain attributes with a decision tree classifier. Individually, the geophysical data were relatively weak predictors of soil information. Using all of the geophysical and terrain data, the soil types were predicted very well, with less than 2% of the area misclassified. Clay et al. [248] empirically derived soil patterns from EC$_a$ readings and elevation data. Generally, well-drained soils in the summit area and poorly-drained soils in the valley bottoms had low and high EC$_a$ values, respectively.

An interesting comparison between EC_a and the soil values of the German national soil inventory (Bodenzahlen) was presented by Neudecker et al. [249]. In 11 fields in four different German regions, R^2 varied between 0.1 and 0.71. Highly heterogeneous fields showed a range of R^2 values from 0.03–0.71. The authors concluded that EC_a measurements were much better in delineating zones of different soil substrates than other, rather subjective methods such as the German national soil inventory.

5. Applications in Agriculture

5.1. Derivation of Agricultural Yield Variability and Management Zones

EC_a is used to reflect crop yields and to derive management zones. Different studies show that crop yields vary due to site-specific differences and temporal climatic changes (Table 6).

Table 6. Composition of literature with derivations of yield maps, management zones and selection of areas for fertilization with EM38-EC_a.

Study	Investigation Object	Location of Investigation
[172]	Yield maps, Soil types and EC_a	Virginia, USA
[106]	EC_a, NIR, elevation, slope with k-means clustering to define management zones	North Carolina, USA
[65]	Help for define management options with EC_a	SW, Australia
[250]	Development of predictors of vine yield from EC_a	New Zealand
[251]	Management zones in viniculture	Clare Valley, Australia
[103]	Relationship EC_a crop yield	North, east Germany
[252]	Management zones on soil NO_3 and P sampling variability	South Dakota, USA
[253,254]	N-management zones	Belgium
[130,199, 255]	Soil properties and cotton yield	California, USA
[174]	Soil pattern as basis of management zones	England
[12]	Identifiing management classes with ECa (measured at high and low water content)	North-east Australia
[154]	Multi-sensor data (EM38, GPR, FieldSpec) to delineate homogeneous zones	Italy
[256]	Relationships EC_a, N-fertilizing demand	Southwest Sweden
[257]	Relationship EC_a crop yield , management zones	Brandenburg, Germany
[258]	Establishing of management zones with Corg, clay, NO_3, K, Zn, EC_a, corn yield data	Colorado, USA
[259]	Correlations ECa with yield, sugar content, piercing force, Kramer energy in a single year	Peleponnese, Greece
[260]	Relationship EC_a crop yield, management zones	Missouri, USA
[261]	Management zones and N applications	Missouri, USA
[262]	Management zones delineation software	Missouri, USA
[224]	EC_a to predict NO_3-concentration	Dakota, USA
[131]	EC_a zones	Nebraska, USA
[263]	Distribution of legumes in pastures in dependence of EC_a and slope	Iowa, USA
[176]	Soil types (derived from EC_a) related to yield, K, Mg	Elbe-Weser-region, Germany
[92]	Management zones salt affected sites	California, USA
[264]	Development of key properties for delineation management zones	North Belgium
[265]	Management zones in a paddy rice field with EC_a	Bangladesh
[226,266]	Relationship EC_a crop yield	Iowa, USA
[267]	Management zones with yield, elevation and EC_a	Iowa, USA
[132]	Relationship EC_a crop yield	Missouri, USA
[268]	ECa-maps to derive management zones	Iowa, USA
[269]	Relationship EC_a crop yield, terrain attributes	Iowa, USA

Table 6. *Cont*.

[213]	Relationship and classification EC$_a$ crop yield	North central Missouri, USA
[270]	Managing and monitoring variability in vineyards	Australia
[271]	Management zones with yield, elevation, EC$_a$, aerial photos	Nebraska, USA
[272]	Site-specific management of grassland	Ireland
[249]	Comparison EC$_a$ – German national soil inventory (Bodenzahlen)	Bavaria, Germany
[273]	Lime applicationto reduce subsoil acidity	Western Australia
[225]	Relationships EC$_a$, N-fertilizing zones	Saxonia, Germany
[274]	Senor application in viticulture	Australia
[275]	Multiyear EC$_a$ – yield relationship	Victoria, Australia
[276]	Delineation of site-specific management-zones with ECa and topographic parameters	Nile Delta, Egypt
[277]	Data fusion (Terrian attributes, EC$_a$, yield, aerial imagers)	Minnesota, USA
[179]	Yield zones, yield per year, in combination with terrain parameters and other sensors	North West Victoria, Australia
[164]	Relationship EC$_a$ crop yield	Bavaria, Germany
[196]	Relationship EC$_a$ crop yield	Missouri, USA
[278]	Relationship ECa − volumetric water content (−35 cm) – yield	NRW, Germany
[279]	EC$_a$ and yield of apples	Ankara, Turkey,
[42,45]	Sampling points with ratio (EC$_{av}$-EM38/EC$_a$-EM31)	NSW, Australia
[245]	Management zones and multilevel sampling scheme	Central Iowa, USA
[280]	Management zones with EC$_a$ relative differences (ϑ_{ij}, Eq. 31)	SW Spain
[104]	Management zones (delineated mainly with subsoil clay from ((EC$_{av}$* EC$_{ah}$)$^{.5}$)) delivered from EC$_a$)	Flanders, Belgium
[281]	Characterization of soil variation by key variables: pH, EC$_a$, organic matter	Flanders, Belgium
[121]	Interpolation of EC$_a$ across field boundaries	Bavaria, Germany
[282]	EC and soil inorganic N (no EM38-EC$_a$)	Nebraska, USA

Management (productivity) zones with similar yields and used by farmers to make application decisions based upon calculations of the expected yield. The applied methods and additional predictors are different in this context. In fact, EC$_a$ has no direct relationship to the growth and yield of plants, but the spatial variation of EC$_a$ is partly correlated with soil properties that do affect crop productivity. Several studies have shown this connection [88,127,213,226,271]. The advantage of EC$_a$ in comparison to yield measurements is its relative temporal stability, which offers a better basis for the delineation of management zones than variable yield mapping information does. With cluster analysis, Fleming et al. [258] confirmed that management zones represented different suites of soil. In one field, soil organic matter, clay, nitrate, potassium, zinc, EC$_a$ and corn yield data corresponded to the levels indicated by the management zones. In a different field, only the medium productivity zone had the highest values for these parameters. Cockx et al. [253,254] used the spatial distribution of NO$_3^-$ in addition to EC$_a$ to create nitrogen management zones. The interpolated EC$_a$ measurements were the input for a fuzzy k means classification. This procedure placed each single point in a membership in each class [46]. The method minimized the multivariate within-class variance, and consequently, individuals in the same class had similar attributes [283]. Using a principle compound analysis, (PCA) Vitharana et al. [189,281] detected the importance of pH, EC$_{a-v}$ and organic matter as independent key variables to characterize overall soil variation. The authors identified and delineated four classes (with a fuzzy k-means algorithm) with these variables. Clear differences in soil properties and landscape positions were found between these classes, and the three-year average standardized yields (grain and straw) were also different across the classes. Schepers et al. [277] aggregated brightness images, elevation, EC$_a$ and yield into management zones using principal component analysis in combination with unsupervised classification. Domsch et al. [257] correlated EC$_a$ and yield within the boundary lines method. In this context, Corwin et al. [284] combined EC$_a$ with leaching of pollutants and Johnson et al. [204] combined EC$_a$ with soil quality parameters (measured as bulk

density, water content, clay content, organic matter, N, extract-able P, pH, microbial biomass C and N, potentially mineralizable N). In an investigation on claypan soil, Sudduth et al. [196] described a negative relationship between EC_a and grain yield in a dry year. The correlations with corn and soybean in a wet year in topographically highly variable landscape were also negative, as observed by Jaynes et al. [226,266]. However, in both studies no significant relationships were observed in years with a more normal water supply. In a newer study of claypan areas, Jung et al. [132] described negative relationships for corn and soybean in years with more than 150 mm precipitation, while in contrast, EC_a was positively correlated in years with less than 150 mm precipitation. In both cases, the correlation coefficients were not higher than 0.74. However, the authors concluded, "while correlation analysis itself is far from a definitive analysis, we suspect this similar pattern (between EC_a and yield) in correlation is not coincidental". Kitchen et al. [213] related EC_a to yield applying boundary line analysis on claypan soils. A significant relationship (boundary lines with $R^2 > 0.25$ on most areas) was apparent, but climate, crop type, and specific field information was also necessary to explain the structure of the potential yield by EC_a interaction. The authors divided the relationships between productivity and EC_a into four categories: (1) positive; (2) negative; (3) positive in some portions of the field and negative in others; and (4) no relationship. The strongest relationships were negative, reflecting the tendency of claypan soils to be water-limited for crop production in the majority of growing seasons [133]. Figure 4 and Table 7 show the relationships between EC_a (EM38 in both configurations) and yield of the long-term field experiment Dürnast 020 (South Germany, (4477221.13E, 5362908.78N), Heil, unpublished).

Table 7. Regressions between EC_a and multi-annual mean of yield (wheat) of the long-term experiment Dürnast 020 in dependence of fertilization level (see Figure 1).

Yield (dt ha^{-1})	Configuration	N	Equation	R^2 Significance
Control plots	Vertical	12	$101.33 - 1.411 \times EC_a$	0.67 ***
	Horizontal	12	$64.61 - 0.758 \times EC_a$	0.81 ***
Fertilized plots (low)	Vertical	42	$106.85 - 0.81 \times EC_a$	0.36 **
	Horizontal	42	$53.466 + 1.394 \times EC_a - 0.025 \times EC_a^2$	0.76 ***
Fertilized plots (high)	Vertical	42	$111.2 - 0.811 \times EC_a$	0.22 *
	Horizontal	42	$76.853 + 0.361 \times EC_a - 0.012 \times EC_a^2$	0.67 ***

n.s. > 0.05, * $0.05 \geq p > 0.01$, ** $0.01 \geq p > 0.001$, *** $p \leq 0.001$.
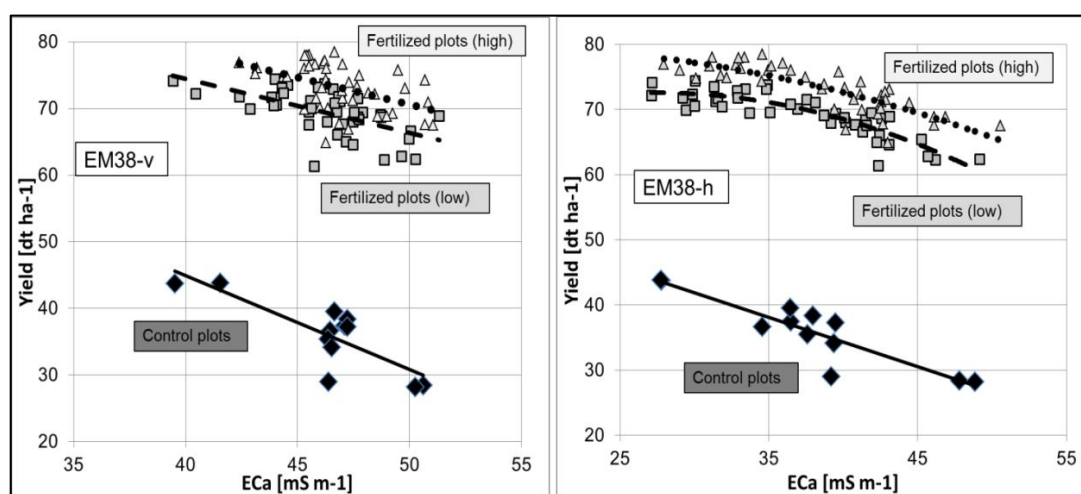

Figure 4. Relationships between EC_a and multi-annual mean of yield (wheat) of the long-term experiment Dürnast 020 in dependence of fertilization level (control plots: no fertilizer, fertilized plots (low): 100–140 kg ha^{-1} N, fertilized plots (high): 150–180 kg ha^{-1} N).

Here the application of different N-fertilizers with two fertilization levels has been tested since 1979. In the Figure 4 the multi annual means of the yields of wheat (1980, 1983, 1986, 1989, 1992, 1995, 1998, 2001, 2004, 2007, 2010, 2012) were divided in the two fertilization levels and the unfertilized control plots. Within this site, soils were mapped as deposits of Pleistocene loess, and the dominating soil types were fine-silty Dystric Eutrochrept and fine-loamy Typic Udifluvent (German Soil Survey, Bodenkundliche Kartieranleitung 2005). On this productive field (plant available water capacity 250 mm until 100 cm depth , C-content: 1.4% (0–30 cm) and 0.4% (50–75 cm)) all relationships are negative with always significant R^2 and also linear or weak quadratic curves. Remarkable is that the curves have similar slopes, at least in the higher ECa range. The always lower coefficients of determination in the case of the vertical configuration could reflect, that the deeper soil is less important to the plant growth.

After a first visual inspection the lowest values of yield correspond with higher contents of clay. The curve progressions allow further interpretations:

- The spatial distribution of the yield was at first influenced by the EC$_a$ across the field. Treatment effects (fertilizing level, fertilizer form) were overlain by soil conditions with different EC$_a$ values.
- The height of the yield was secondly assumedly determined by the level of fertilization.

In claypan soils, Fraisse et al. [260] also used a combination of EC$_a$ and topographic features (with unsupervised classification) to develop zones and evaluated their ability to describe yield variability. By dividing a field into four or five zones based on EC$_a$, slope, and elevation, 10% to 37% of corn and soybean yield was explained. In this context, Fridgen et al. [262] described software with a similar derivation of the subfield management zone. Kitchen et al. [285] used unsupervised fuzzy-k-means clustering to delineate productivity zones with EC$_a$ and elevation measurements on claypan soils. Productivity zones were also derived by Jaynes et al. [267] based on a series of profiling steps in combination with cluster analysis to determine the relationship between yield clusters and easily measured terrain attributes (i.e., slope, plane curvature, aspect, depth of depression) and EC$_a$. In contrast to the previous investigations, Kilborn et al. [269] found no strong relationships between elevation, slope, and soil EC$_a$ with respect to biomass yield and composition. The results of Bang [106] indicate that clustering with EC$_a$ and NIR surveys could be used to delineate management zones that characterize spatial variations in soil chemical properties. However, these zones were less consistent for characterizing spatial variability in yields across temporal water content variation. Furthermore, the author reported that clustering zones developed from EC$_a$ values measured under relatively dry conditions were particularly effective in partitioning the spatial variability of SOM. It is clear that zones developed from clustering elevation and bare-soil NIR radiance were more effective than EC$_a$ alone in capturing variability in K, CEC, and SOM. Clustering on EC$_a$ with elevation and NIR provided better zones for these parameters and somewhat reduced the variability associated with measuring EC$_a$ under different soil water conditions [106].

A similar praxis was used by Schepers et al. [277]; Chang et al. [252] and Fridgen et al. [262]. Cluster analysis of an EC$_a$ map alone or with auxiliary data, such as terrain attributes and bare-soil images, has been widely used to delineate soil-based management zones. The relationship between EC$_a$ measurements, soil properties and sugar beet yields in salt-affected soils was studied by Kaffka et al. [20]. In these soils, yield was most highly correlated with salinity. This work demonstrated the utility of relationships between EC$_a$ and crop yield to answer resource input questions. Rampant and Abuzar [286] predicted yield zones from a combination of geophysical (i.e., EM38, EM31, airborne gamma radiometrics) and terrain attributes with a decision tree classifier. Individually, the geophysical data were relatively poor predictors of the yield zones. The combination of all sensors and terrain data could predict yield zones quite well, misclassifying only 5% of the area. The predictions of yield for an individual year were always worse for yield zones.

The purpose of the application of the EM38 by Guretzky et al. [263] was to examine the relationship of the relief parameter "slope", EC$_a$, and legume distribution in pastures. The authors concluded that slope and EC$_a$ data were useful in selecting sites in pastures with higher legume yield and showed a potential for use in site-specific management of pastures. Dang et al. [12] used an

interesting procedure for identifying management zones on a salinity-affected field. Two surveys of EC$_a$ measurements were carried out; the first used a relatively wet soil profile (April–May 2009) to represent the drained upper limit of soil water, and the second used a relatively dry profile (October–November 2009) to represent the lower limit of soil water content extraction following the harvest of the winter crop. The authors developed a framework to estimate the monetary value of site-specific management options through: (1) identification of potential management classes formed from EC$_a$ at lower limit of soil water content; (2) measurement of soil attributes generally associated with soil constraints in the region; (3) grain yield monitoring; and (4) simple on-farm experiments.

Islam et al. [264] estimated key properties to identify management zones on loess and sandy soils. The authors identified EC$_a$, topsoil pH, and elevation as key properties, which were used to delineate management classes and to construct an excellent multiple regression model between yield and the key properties. Additionally, Islam et al. [265] described the construction of waterproofed housing for the EM38, which was built using PVC pipes for swimming in a paddy rice field. The EC$_a$ data were classified into three classes with the fuzzy k-means classification method. The variation among the classes was related to differences in subsoil bulk density. The smallest EC$_a$ values representing the lowest yield and also the lowest bulk density.

There was also a significant difference in rice yield among the EC$_a$ classes, with Vanderlinden et al. [280] carried out a procedure for characterizing a management system. EC$_a$ patterns expressed as relative differences (ϑ_{ij}) were associated with topography, soil depth and soil structure, and the authors derived management zones with principal component analysis.

A very detailed insight into the relationship between EC$_a$ and yield was given by Robinson et al. [275] for sites in Victoria, Australia. However, the multi-year measurements of yield and EC$_a$ delivered an inconsistent picture. Significant influences of EC$_a$ on yield were found for all measurements, but they evidenced alternating directions in semi-arid and rainy environments. (1) Decreasing yield was combined with increasing EC$_{a-v}$ when texture-contrast and gradational soils with shallow topsoils occurred along with increasing clay content and physio-chemical constraints; (2) In soils without significant texture-contrast, in which physio-chemical conditions were more favourable for water in the subsoil, higher yields resulted; (3) Positive trends of EC$_a$ and yield were attributed to the occurrence of higher plant-available water in the root zone in high and moderate yield zones. However, the *R*^{2} did not exceed 0.15 for all calculations.

Additionally, the EM38 has been applied in vineyards for describing soil variability to an increasing extent [5,15–57,62,70–82,86,90–93,95–270]. Bramley et al. [250] described a close relationship between EC$_a$ readings from stony shallow soils and trunk circumference. However, sufficient predictors for vine vigour were not found in these investigations.

EM38 has more rarely been applied to apple orchards. Türker et al. [279] produced EC$_a$ maps and compared them with yield and pomological characteristic maps. As a result, the highest value of a non-linear regression between EC$_a$ and apple yield was determined with an *R*^{2} of 0.94.

5.2. Improvement of the Efficiency of Agricultural Field Experimentation

Only a few publications reported about the application of EC$_a$ readings to improve the efficiency of field experiments. An accurate comparison of treatments within agricultural field experiments is the primary objective of these evaluations. Spatial soil variability can have adverse effects on the accuracy and efficiency of such trials (Table 8).

Table 8. Applications of EM38-EC$_a$ for improving the efficiency of field experiments.

Study	Investigation Object	Location of Investigation
[173]	EC$_a$ to derive more homogeneous lacustrine-derived soils	Iowa, USA
[204]	Classification parameter for block design	California, USA
[287]	P-content in a field experiment with different levels of manure applications	Michigan, USA
[288]	Comparison of yield between strip trials, partly EC$_a$; simplified evaluation method	South, west Australia

Kravchenko et al. [289] used EC_a as a covariate to improve the accuracy of P values on field with different levels of manure applications. Standard errors for the means of P with EC_a as a covariate were smaller than those for which EC_a was not used as a covariate. In soils with medium and high EC_a values, the control treatment (no manure) had a significantly lower P concentration.

Johnson et al. [204] applied field wide EC_a readings as a classification parameter for a block design. Blocks were located in homogeneous areas based upon measurements of soil parameters that are significant for yield. The authors noted that EC_a classification can be used as a basis for blocking only when EC_a and yield are correlated. On these sites, which were described by Johnson et al. [204], the dominating factors were salinity and clay content. The authors described the application of EC_a as a "compelling tool in statistical design".

The initial point of the publication of Lawes and Bramley [288] is the fact that farmers and their advisers are often not able to implement methods that are necessary for evaluation trials on their farms. The authors explore a new and simple approach to the analysis of farmer strip trials and the spatial variability of treatment response. Yield data descriptions with a linear model that accounted for the spatial autocorrelation in the data and a moving pairwise comparison of treatments were applied by the authors. The results suggest that the pairwise comparison adequately identified treatment differences and their significance. This method can be readily implemented and expanded with EC_a readings, and it offers an important advance to facilitate on-farm experimentation using precision agriculture technologies.

Brevik et al. [173] indicated a need to investigate the application of EC_a techniques in fields with more homogenous soil properties. For these investigations, the authors selected a field with lacustrine-derived soils that exhibited only weak spatial variability in soil properties. The highly uniform EC_a readings obtained did not allow differentiation of soil map units with the EC_a data. However, the results did confirm the uniform nature of the soils in the field, a critical criterion for precision agriculture applications. An example of the application of conductivity values is given in Table 9 [4].

Table 9. Simulation of the yield (1980–2012) with ANOVA and ANCOVA with the factors fertilizing level and fertilizer-no. and the covariates ECa and relief parameters.

Target Variable, Years	Model and Effects	Significance	Partial Eta-Square	Adjusted R^2	RMSE (dt ha^{-1})
Yield (dt ha $^{-1}$), mean 1980, 1983, 1986, 1989, 1992, 1995, 1998, 2001, 2004, 2007, 2010, 2012	Adjusted model	0.008	0.313		
	Constant	0.000	0.998		
	Fertilization level	0.000	0.258	0.18	3.26
	Fertilizer no.	0.414	0.081		
	Fertilization level*Fertilizer no.	0.971	0.018		
Yield (dt ha $^{-1}$)^3, mean (1980, 1983, 1986, 1989, 1992, 1995, 1998, 2001, 2004, 2007, 2010, 2012	Adjusted model	0.000	0.904		
	Constant	0.007	0.106		
	Fertilization level	0.000	0.764		
	Fertilizer no.	0.000	0.341		
	Fertilization level* Fertilizer no.	0.145	0.131	0.88	1.29
	ECa (EM38-h)^3	0.000	0.275		
	lg10(ECa (EM38-v))	0.000	0.276		
	Channelnetwork^3	0.001	0.144		
	TWI^3	0.024	0.075		

Significance: n.s. > 0.05,   * $0.05 \geq p > 0.01$, ** $0.01 \geq p > 0.001$, *** $p \leq 0.001$; Partial eta-square: Measure of sensitivity to the correlated independent variables; Adjusted R^2: adjusted R^2 (coefficient of determination).

The relationships presented in Section 5.1 between EC_a and yield are here integrated in a variance of analysis (ANOVA) and an analysis of covariance (ANCOVA) with the target to model the multi-annual yield of the long-term experiment Dürnast 020. In the ANOVA only the factors

"fertilizing level" and "the form of fertilizer" have been considered. To enhance the accuracy of the simulation the covariates EC_a as well as topographical parameters have been added. The ANOVA procedure delivers with the fertilization level as the single influencing factor only a weak result ($R^2 = 0.185$, RMSE = 3.26 dt ha^{-1}). In contrast to this result the application of the ANCOVA introduced the factors fertilization level and fertilization no. and the covariate EC_a (EM38-h and EM38-v) in the simulation. The R^2 of 0,875 and a RMSE with 1.29 dt ha^{-1} indicate a severe enhancement in comparison to the ANOVA. The partial eta-square illustrates that the introduction of the EC_a readings was the main reason of this improvement. The topographical parameter channelnet (channel network base level (-)) and TWI (topographical wetness index (-)) had only minor meaning.

Here, EC_a has been shown to be a useful indicator of soil variability. Compared to the standard analysis ANOVA, an ANCOVA with EC_a as covariate (and also topographical parameters) reduced RMSE and enhanced R^2 for treatment means and improved the accuracy of this field experiment.

5.3. Additional Application of EM38 in Agriculture and Horticulture

Additionally, some publications describe the use of EC_a to assess environmental susceptibility and/or effects (Table 10).

Table 10. Additional applications of EM38-EC_a in agriculture and horticulture.

Study	Investigation Object	Location of Investigation
[234]	Corg, K, pH, Bray-2 P,	Louisiana, USA
[290]	Detecting soil properties as indicators for population density of Redheaded cockchafer (*Adoryphourus couloni*)	Victoria, Australia
[215,217, 219]	Specific ions that are associated with animal waste	Nebraska, USA
[220]	N decomposition, organic and artificial fertilizer	Nebraska, USA
[221]	EC_a as an indicator of N gains and losses, available N sufficiency for corn in early stage and NO3-N surplus after harvest	Nebraska, USA
[291]	EC_a as indicator for soil conditions which are prefered by *Heterodera schachtii*	North Rhine-Westphalia, Germany
[292]	Herbicide partition coefficients	Iowa, USA
[233]	Variation in soil testing P	Missouri, Oklahoma, USA
[293]	Part of fungicide application models in combination with ratio vegetation index	Denmark
[294]	Weed distribution, herbicide injury in dependency of EC_a	North Rhine-Westphalia, Germany
[222]	NH$_4$, K in animal slurries	Ireland

Jaynes et al. [292] correlated EC_a readings with herbicide partition coefficients. The maps are useful for determining areas with a higher leaching potential for herbicide (atrazine) application. Olesen et al. [293] developed two different algorithms (an empirical model and a causal model) for spatially varying fungicide applications. Both models make use of a ratio vegetation index and EM38 measurements. EC_a maps describe the soil characteristics, in particular the soil clay content.

Hbirkou et al. [291] used EC_a maps for constructing relationships between ECa and the beet cyst nematode, *Heterodera schachtii*. This nematode prefers deep soil with medium to light soil and non-stagnic water conditions. Correlations between EC_a and nematode population density were moderate ($R^2 = 0.47$) and strong ($R^2 = 0.74$). Management maps based on EC_a and soil taxation maps indicated areas with different soil-related living conditions for H. schachtii. These maps could make farmers able to improve site-specific management strategies on nematode-infested fields.

Grigera et al. [131] created four EC_a zones from EC_a readings, based on ranges of both configurations using an unsupervised classification. Soil microbial groups were correlated with different soil C fractions in the upper soil (−15 cm) and were similar across EC_a zones. Zone distribution and biomarkers correlated in dependence of the fractions of particulate organic matter (fine particulate organic matter: bacterial (R = 0.85), actinomycetes (R = 0.71) biomarker

concentrations; coarse particulate organic matter: bacteria $R = 0.69$, actinomycetes $R = 0.48$). In contrast, fungal ($R = 0.77$) and mycorrhizal ($R = 0.48$) biomarker concentrations were correlated only with coarse organic matter.

6. Application of EM38 in Archaeology

The application of the EM38 device is not restricted to soil properties; it also detects extrinsic components (Table 11).

Table 11. Additional applications of EM38-EC$_a$ in archaeology.

Study	Investigation Object	Location of Investigation
[295]	Detection of graves with inphase and quadphase readings	Maryland, USA
[296,297]	Prehistoric earthworks with measurements in inphase mode	Ohio, USA
[298]	Metal objects from the 18th century	Canada
[299]	Removing of the effect of elevation on the distribution of EC$_a$ readings	Santa Catarina State, Brazil
[300]	Comparison EM38 fluxgate gradiometer	Belgium
[301]	Medieval manor in the dutch polders	Netherlands
[302]	Area prospection with EM38 and MS2D	Tundra region, Sweden

Ferguson [298] applied EC$_a$ values to find metal objects in a settlement area from the 18th century. Measurements of EC$_a$ also appear to be suitable to search for graves [303]. Low values can indicate a proximity to metal, but high conductivity has been associated with grave shafts at one cemetery.

A more sophisticated procedure for archaeological detections was described by Dalan and Bevan [296]. An EM38 meter, which was operated in the inphase mode, measured the susceptibility of the top half-meter of soil. This susceptibility sounding was performed using a series of heights from 2 m to the surface, with readings taken at intervals of 5 cm. These measurements were analysed with the aid of the depth sensitivity function of McNeill [304]. In this manner, the authors could detect magnetic layers to a depth of 50 cm.

Viberg et al. [302] combined the EM38 with the MS2D (Bartington MS2 magnetic susceptibility meter). The anomalies contained in the survey data were explained by the subsequent archaeological excavation. A rubbish pit which consist mainly of organic material and fire-cracked stones was detected in both the MS2D and EM-38 data. This study of Simpson et al. [301] used additionally a fluxgate gradiometer measurements on an archaeological site. The results of the first survey showed very strong magnetic anomalies in the central field, which were caused by the brick remains of the castle. The most useful results with the EM38 were obtained from the magnetic susceptibility. Its anomalies corresponded well with the gradiometer anomalies. To enhance EC$_a$ maps, Santos et al. [299] recommended a simple procedure to eliminate the effect of elevation on EC$_a$. In the experience of the authors, soil anomalies are partly changed by changing the elevation within an investigation area according to the water table depth or the conductive sediment layer. With a linear dependence between conductivity and the site elevation the influence of topography was removed. Corrected EC$_a$ maps substantially improved the recognition of anomalies. These maps also show a greater similarity with magnetic susceptibility maps, with both identifying archaeological structures of interest: a well-structured fireplace and a concentration of ceramic fragments.

7. Conclusions and Closing Remarks

There is no doubt that EM38 measurements have an increasing importance in exploration of areas, but weaknesses/unclarities of the method are also described in the literature:

- The interpretation and utility of EC$_a$ readings are highly location and soil-specific; the soil properties contributing to EC$_a$ measurements must be clearly understood. From the various calibration results, it appears that regression constants for relationships between EC$_a$, EC$_e$, soil texture, yield, etc. are not necessarily transferable from one region to another. Several factors

affect the strength of the signal and therefore, the relationships. In addition to texture, salt concentration and other physicochemical properties, calibrations are further affected by the relative response of the signal according to depth, the non-linearity of the signal and the collinearity between horizontal and vertical readings. The soil parameter with the greatest influence on EC_a is also the best derivable.

- Only a few authors [108,196] account for the influence of the farming system, crop biomass, applications of fertilizer at the time of measurement on EC_a distributions. Most of the identified soil parameters that influence EC_a have significant interdependency and can thus provide multivariate effects on EC_a.

- The modelling of EC_a, soil properties, climate and yield are important for identifying the geographic extent to which specific applications of EC_a technology (e.g., EC_a – texture relationships) can be appropriately applied.

- In the case of detecting salinity, obviously better results are achieved if both EM38 readings (vertical and horizontal) are combined with EC_e values from different depth ranges. Nevertheless, Vlotman et al. [305] posed the question about the need for converting the EC_e from EC_a. As McKenzie [24,25] showed, a classification of salinity tolerance level of different crops is also possible only with EM38 readings. A partitioning in areas of low, medium and high salinity with measurements in a single mode or with a combination of v- and h-mode is often a sufficient inventory of the salinity distribution. But it is necessary to take into account, that on the one field e.g., 60 mS m^{-1} has salt problems while another field with the same reading does not have such problems. Therefore EC_e will continue to be important at least in the near future.

- The quality of a regression is often determined by a sufficient range of dependent and independent variables. Delin and Söderström [124] noted that when the EC_a data were correlated with the clay content over the whole farm, the result was much better then when the correlation was restricted to single zones. This quality is also better if the target variable is also the dominant EC_a-influencing factor.

- The construction of soil sampling designs with EC_a readings is limited to those properties that correlate with EC_a. Other parameters require some other sampling approach such as random, grid, or stratified random sampling.

The world-wide application of the EM38 (and also of other soil sensors) is very varying:
- It seems that the detection of salinity is still the main area of application.
- Site-specific management in agriculture with the application of EC_a is still in Germany in an initial phase of adoption among farmers. Predicting the future is difficult. Nonetheless, a greater presence of site-specific crop management based on soil detection is to be hoped for.
- Furthermore in Germany increases the investigations in improving soil maps and in detecting soil functions, including: plant available water, sorption capacity, binding strength for heavy metals, filtering of unbound substances and natural soil fertility. Additionally, soil protection measures are also indicators for erosion prevention, retention of nutrients, and conservation/enhancement of carbon contents (based on good agricultural practice after Article 17, German Soil Protection Act). The selection of soil functions is based on the German Soil Protection Act (LABO—Bund-Länder-Arbeitsgemeinschaft Bodenschutz). Here it is not common sense to carry out this also with EM38. Until now it is not well known that, compared to traditional soil survey methods, EM38 readings can more effectively characterize diffuse soil boundaries and identify areas of similar soils within mapped soil units. This gives soil scientists greater confidence in their soil mapping.
- The application in forests is world-wide rather seldom. But also here is an enormous potential to improve the existing site maps and to test the water distribution between the trees.
- The improvement of evaluation of field experiments with EC_a readings as covariate is more rarely used. The spatial variability of soil properties can have adverse effects on the accuracy and efficiency of field experiments. Here is a great potential to take into account the soil conditions by using ECa readings.

- The fusion of the data of other sensors also shows great potential. The idea behind the combination of proximal soil sensors is that the accuracy of a single sensor is often not sufficient. The reading of one sensor is affected by more than one soil property of interest. The fusion of sensor data can overcome this weakness by extracting complementary information from multiple sensors or sources. Until now to an increasing extent, the readings of EM38 are evaluated in combination mainly with VIS–NIR and a gamma-ray-spectrometer.
- Many of the instruments measure at the point or sample scale, such as soil moisture probes and tensiometers, while remote sensing devices determine regional patterns. But these techniques are limited in the depth of penetration into the subsurface.

Here geophysical methods have a positive impact, obtaining data at a range of spatial scales across fields. This survey has shown that considerable progress has been made in detection and understanding of soil functions within the last decades. Applications of practical sensors such as the EM38 are needed to achieve sustainable agriculture, to optimize economic return and to protect the environment, especially the soil.

Conflicts of Interest: The authors declare no conflicts of interest.

Abbreviations

CEC	Cation exchange capacity
EC_a	Apparent electrical conductivity
EC_{av}	Apparent electrical conductivity, measured in vertical mode
EC_{ah}	Apparent electrical conductivity, measured in horizontal mode
EC_e	Electrical conductivity of aqueous soil extracts $EC_{1:5}$, $EC_{1:2}$ or $EC_{1:1,}$ soil/water suspensions)
EC_P	EC_a calculated by using predictive equations
EC_{ref}	Quotient of the measured EC_a and the EC
θ_v, θ_w	Weighted water content after vertical and horizontal mode
Z	Soil depth

References

1. Sudduth, K.A.; Drummond, S.T.; Kitchen, N.R. Accuracy issues in electromagnetic induction sensing of soil electrical conductivity for precision agriculture. *Comput. Electron. Agric.* **2001**, *31*, 239–264.
2. Doolittle, J.A.; Brevik, E.C. The use of electromagnetic induction techniques in soils studies. *Geoderma* **2014**, *223–225*, 33–45.
3. Sudduth, K.A.; Kitchen, N.R.; Wiebold, W.J.; Batchelor, W.D. Relating apparent electrical conductivity to soil properties across the north-central USA. *Comput. Electron. Agric.* **2005**, *46*, 263–283.
4. Heil, K.; Schmidhalter, U. Comparison of the EM38 and EM38-MK2 electromagnetic induction-based sensors for spatial soil analysis at field scale. *Comput. Electron. Agric.* **2015**, *110*, 267–280.
5. McNeill, J. Electromagnetic Terrain Conductivity Measurement at Low Induction Numbers. Available online: http://www.geonics.com/pdfs/technicalnotes/tn6.pdf (accessed on 1 November 2017).
6. Geonics Limited. Ground Conductivity Meters. Available online: http://www.geonics.com/html/conductivitymeters.html (accessed on 15 August 2017).
7. Corwin, D.L., Lesch, S.M., Apparent soil electrical conductivity measurements in agriculture. *Comput. Electron. Agric.* **2005**, *46*, 11–43.
8. Cassel, F.; Goorahoo, D.; Sharmasarkar, S. Salinization and Yield Potential of a Salt-Laden Californian Soil: An In Situ Geophysical Analysis. *Water Air Soil Pollut.* **2015**, *226*, 1–8.
9. Cook, P.G.; Walker, G.R. Depth Profiles of Electrical-Conductivity from Linear-Combinations of Electromagnetic Induction Measurements. *Soil Sci. Soc. Am. J.* **1992**, *56*, 1015–1022.
10. Corwin, D.; Rhoades, J. An improved technique for determining soil electrical conductivity-depth relations from above-ground electromagnetic measurements. *Soil Sci. Soc. Am. J.* **1982**, *46*, 517–520.

11. Corwin, D.; Rhoades, J. Measurement of inverted electrical conductivity profiles using electromagnetic induction. *Soil Sci. Soc. Am. J.* **1984**, *48*, 288–291.

12. Dang, Y.P.; Dalal, R.C.; Pringle, M.J.; Biggs, A.J.W.; Darr, S.; Sauer, B.; Moss, J.; Payne, J.; Orange, D. Electromagnetic induction sensing of soil identifies constraints to the crop yields of north-eastern Australia. *Soil Res.* **2011**, *49*, 559–571.

13. Doolittle, J.; Petersen, M.; Wheeler, T. Comparison of two electromagnetic induction tools in salinity appraisals. *J. Soil Water Conserv.* **2001**, *56*, 257–262.

14. Dunn, G.; Taylor, D.; Nester, M.; Beetson, T. Performance of twelve selected Australian tree species on a saline site in southeast Queensland. *For. Ecol. Manag.* **1994**, *70*, 255–264.

15. Ghany, A.H.; Omara, A.M.; El Nagar, M.A. *Testing Electromagnetic Induction Device (EM 38) Under Egyptian Conditions*; Vlotman, W.F., Ed.; EM38 Workshop: New Delhi, India.

16. Gill, H.S.; Yee, M. EM-38 for Assessing Surface and Sub-Soil Salinity and Its Relationship to Establishment and Growth of Selected Perennial Pasture Species. In Proceedings of the SuperSoil 2004—3rd Australian New Zealand Soils Conference, Sydney, Australia, 5–9 December 2004.

17. Herrero, J.; Ba, A.; Aragüés, R. Soil salinity and its distribution determined by soil sampling and electromagnetic techniques. *Soil Use Manag.* **2003**, *19*, 119–126.

18. Li, H.; Li, F.; Shi, Z.; Huang, M. Three Dimensional Variability of Soil Electrical Conductivity Based on Electromagnetic Induction Approach. In Proceedings of the 2010 International Conference on Artificial Intelligence and Computational Intelligence (AICI), Sanya, China, 23–24 October 2010; pp. 219–223.

19. Johnston, M.A.; Savage, M.J.; Moolman, J.H.; du Plessis, H.M. Evaluation of calibration methods for interpreting soil salinity from electromagnetic induction measurements. *Soil Sci. Soc. Am. J.* **1997**, *61*, 1627–1633.

20. Kaffka, S.R.; Lesch, S.M.; Bali, K.M.; Corwin, D.L. Site-specific management in salt-affected sugar beet fields using electromagnetic induction. *Comput. Electron. Agric.* **2005**, *46*, 329–350.

21. Lesch, S.M.; Rhoades, J.D.; Lund, L.J.; Corwin, D.L. Mapping Soil-Salinity Using Calibrated Electromagnetic Measurements. *Soil Sci. Soc. Am. J.* **1992**, *56*, 540–548.

22. McNeill, J.D. Rapid, accurate mapping of soil salinity by electromagnetic ground conductivity meters. *Adv. Meas. Soil Phys. Prop. Bring. Theory Pract.* **1992**, 209–229.

23. McKenzie, R.C.; Chomistek, W.; Clark, N.F. Conversion of Electromagnetic Inductance Readings to Saturated Paste Extract Values in Soils for Different Temperature, Texture, and Moisture Conditions. *Can. J. Soil Sci.* **1989**, *69*, 25–32.

24. McKenzie, R.C.; Mathers, H.M.; Woods, S.A. *Salinity and Crop Tolerance of Ornamental Trees and Shrubs*; Alberta Special Crops and Horticultural Research Center: Brooks, AB, Canada, 1993.

25. McKenzie, R.C.; George, R.J.; Woods, S.A.; Cannon, M.E.; Bennett, D.L. Use of the Electromagnetic-Induction Meter (EM38) as a Tool in Managing Salinisation. *Hydrogeol. J.* **1997**, *5*, 37–50.

26. McKenzie, R.C. Salinity: Mapping and Determining Crop Tolerance with an Electromagnetic Induction Meter (Canada). Available online: http://www2.alterra.wur.nl/Internet/webdocs/ilri-publicaties/special_reports/Srep13/Srep13-h6.pdf (accessed on 1 November 2017).

27. Nettleton, W.D.; Bushue, L.; Doolittle, J.A.; Endres, T.J.; Indorante, S.J. Sodium-Affected Soil Identification in South-Central Illinois by Electromagnetic Induction. *Soil Sci. Soc. Am. J.* **1994**, *58*, 1190–1193.

28. Nogues, J.; Robinson, D.A.; Herrero, J. Incorporating electromagnetic induction methods into regional soil salinity survey of irrigation districts. *Soil Sci. Soc. Am. J.* **2006**, *70*, 2075–2085.

29. Norman, C.P. Kyvalley [Victoria] EM38 Salinity Survey. Available online: http://agris.fao.org/agris-search/search.do?recordID=AU9430080 (accessed on 1 November 2017).

30. Norman, C.P. *Training Manual on the Use of the EM38 for Soil Salinity Appraisal*; Victorian Department of Agriculture and Rural Affairs: Victoria, Australia, 1990.

31. Rhoades, J.; Corwin, D. Determining soil electrical conductivity-depth relations using an inductive electromagnetic soil conductivity meter. *Soil Sci. Soc. Am. J.* **1981**, *45*, 255–260.

32. Rhoades, J.D.; Manteghi, N.A.; Shouse, P.J.; Alves, W.J. Soil Electrical-Conductivity and Soil-Salinity—New Formulations and Calibrations. *Soil Sci. Soc. Am. J.* **1989**, *53*, 433–439.

33. Rhoades, J.D.; Chanduvi, F.; Lesch, S. *Soil Salinity Assessment: Methods and Interpretation of Electrical Conductivity Measurements*; FAO—Land and Water Development Divison: Rome, Italy, 1999; p. 166.

34. Rhoades, J.D.; Corwin, D.L.; Lesch, S.M. Geospatial measurements of soil electrical conductivity to assess soil salinity and diffuse salt loading from irrigation. In *Assessment of Non-Point Source Pollution in the Vadose Zone*; Amer Geophysical Union: Washington, DC, USA, 1999; pp. 197–215.

35. Rahimian, M.H.; Hasheminejhad, Y. Calibration of electromagnetic induction device (EM38) for soil salinity assessment. Iranian J. *Soil Res.* **2011**, 44, 243–252.

36. SriRanjan, R.; Karthigesu, T. Evaluation of an electromagnetic method for detecting lateral seepage around manure storage lagoons. ASAE paper No. 952440. American Society of Agricultural Engineers: St. Joseph, MI, USA, 1995.

37. Sharma, D.P.; Gupta, S.K. Application of EM38 for Soil Salinity Appraisal: An Indian Experience. Available online: http://content.alterra.wur.nl/Internet/webdocs/ilri-publicaties/special_reports/Srep13/Srep13-h3.pdf (accessed on 1 November 2017).

38. Slavich, P.; Petterson, G. Estimating average rootzone salinity from electromagnetic induction (EM-38) measurements. *Soil Res.* **1990**, *28*, 453–463.

39. Slavich, P. Determining ECa-depth profiles from electromagnetic induction measurements. *Soil Res.* **1990**, *28*, 443–452.

40. Soliman, A.S.; Farshad, A.; Sporry, R.J.; Shrestha, D.P. Predicting salinization in its early stage, using electro magnetic data and geostatistical techniques: A case study of Nong Suang district, Nakhon Ratchasima, Thailand. In Proceedings of the 25th Asian Conference on Remote Sensing, Chiang Mai, Thailand, 22–26 November 2004.

41. Sheets, K.R.; Taylor, J.P.; Hendrickx, J.M.H. Rapid Salinity Mapping by Electromagnetic Induction for Determining Riparian Restoration Potential. *Restor. Ecol.* **1994**, *2*, 242–246.

42. Triantafilis, J.; Huckel, A.I.; Mcbratney, A.B. Use of a Mobile Electromagnetic Sensing System for Assessment of Soil Salinity and Irrigation Efficiency. In Proceedings of the 16th World Conference of Soil Science, Montpelliers, France, 20–26 August 1998.

43. Triantafilis, J.; Laslett, G.M.; McBratney, A.B. Calibrating an electromagnetic induction instrument to measure salinity in soil under irrigated cotton. *Soil Sci. Soc. Am. J.* **2000**, *64*, 1009–1017.

44. Triantafilis, J.; Huckel, A.I.; Odeh, I.O.A. Comparison of statistical prediction methods for estimating field-scale clay content using different combinations of ancillary variables. *Soil Sci.* **2001**, *166*, 415–427.

45. Triantafilis, J.; Ahmed, M.F.; Odeh, I.O.A. Application of a mobile electromagnetic sensing system (MESS) to assess cause and management of soil salinization in an irrigated cotton-growing field. *Soil Use Manag.* **2002**, *18*, 330–339.

46. Triantafilis, J.; Huckel, A.I.; Odeh, I.O.A. Field-scale assessment of deep drainage risk. *Irrig. Sci.* **2003**, *21*, 183–192.

47. Triantafilis, J.; Odeh, I.O.A.; Jarman, A.L.; Short, M.G.; Kokkoris, E. Estimating and mapping deep drainage risk at the district level in the lower Gwydir and Macquarie valleys, Australia. *Aust. J. Exp. Agric.* **2004**, *44*, 893–912.

48. Vaughan, P.J.; Lesch, S.M.; Corwin, D.L.; Cone, D.G. Water-Content Effect on Soil-Salinity Prediction—A Geostatistical Study Using Cokriging. *Soil Sci. Soc. Am. J.* **1995**, *59*, 1146–1156.

49. Vlotman, W.F. Calibrating the EM38. Available online: http://agris.fao.org/agris-search/search.do?recordID=NL2001003220 (accessed on 1 November 2017).

50. Whiteley, R.J. Environmental geophysics: Challenges and perspectives. *Explor. Geophys.* **1994**, *25*, 189–196.

51. Williams, B.G.; Baker, G. An electromagnetic induction technique for reconnaissance surveys of soil salinity hazards. *Soil Res.* **1982**, *20*, 107–118.

52. Williams, B.G.; Fidler, F.T. The Use of Electromagnetic Induction for Locating Subsurface Saline Material. *IAHS* **1985**, 189–196.

53. Williams, B.; Braunach, M. The Detection of Subsurface Salinity within the Northern Slopes Region of Victoria, Australia. In *Salinity in watercourses and reservoirs : proceedings of the 1983 International Symposium on State-of-the-Art Control of Salinity, July 13-15, 1983, Salt Lake City, Utah*, French, R.H., Ed.; Butterworth Publishers: Stoneham, MA, USA, 1984; pp. 515–524.

54. Wittler, J.M.; Cardon, G.E.; Gates, T.K.; Cooper, C.A.; Sutherland, P.L. Calibration of electromagnetic induction for regional assessment of soil water salinity in an irrigated valley. *J. Irrig. Drain. Eng.—ASCE* **2006**, *132*, 436–444.

55. Wollenhaupt, N.C.; Richardson, J.L.; Foss, J.E.; Doll, E.C. A Rapid Method for Estimating Weighted Soil-Salinity from Apparent Soil Electrical-Conductivity Measured with an Aboveground Electromagnetic Induction Meter. *Can. J. Soil Sci.* **1986**, *66*, 315–321.

56. Yao, R.J.; Yang, J.S.; Liu, G.M. Calibration of soil electromagnetic conductivity in inverted salinity profiles with an integration method. *Pedosphere* **2007**, *17*, 246–256.

57. Zhang, H.; Schroder, J.L.; Pittman, J.J.; Wang, J.J.; Payton, M.E. Soil salinity using saturated paste and 1:1 soil to water extracts. *Soil Sci. Soc. Am. J.* **2005**, *69*, 1146–1151.

58. Chaudhry, M.R.B.A. *Electromagnetic Induction Device (EM38) Calibration and Monitoring Soil Salinity/Environment (Pakistan)*; Vlotman, W.F., Ed.; EM38 Workshop: New Dehli, India, 2000; pp. 37–48.

59. Amezketa, E. Soil salinity assessment using directed soil sampling from a geophysical survey with electromagnetic technology: A case study. *Span. J. Agric. Res.* **2007**, *5*, 91–101.

60. Arndt, J.L.; Prochnow, N.D.; Richardson, J.L. *Estimating Weighted Soil Salinity of Medium Textured Soils in Eastern North DAKOTA with an Aboveground Electromagnetic Induction Meter*; Department of Soil Science, North Dakota State University: Fargo, ND, USA, 1987.

61. Bakker, D.; Hamilton, G.; Hetherington, R.; Spann, C. Productivity of waterlogged and salt-affected land in a Mediterranean climate using bed-furrow systems. *Field Crops Res.* **2010**, *117*, 24–37.

62. Corwin, D.L.; Lesch, S.M. A simplified regional-scale electromagnetic induction—Salinity calibration model using ANOCOVA modeling techniques. *Geoderma* **2014**, *230–231*, 288–295.

63. Akramkhanov, A.; Brus, D.J.; Walvoort, D.J.J. Geostatistical monitoring of soil salinity in Uzbekistan by repeated EMI surveys. *Geoderma* **2014**, *213*, 600–607.

64. Barbiero, L.; Cunnac, S.; Mane, L.; Laperrousaz, C.; Hammecker, C.; Maeght, J.L. Salt distribution in the Senegal middle valley—Analysis of a saline structure on planned irrigation schemes from N'Galenka creek. *Agric. Water Manag.* **2001**, *46*, 201–213.

65. Bennett, D.L.; George, R.J.; Whitfield, B. The use of ground EM systems to accurately assess salt store and help define land management options, for salinity management. *Explor. Geophys.* **2000**, *31*, 249–254.

66. Broadfoot, K.; Morris, M.; Stevens, D.; Heuperman, A. The role of EM38 in land and water management planning on the Tragowel Plains in Northern Victoria. *Explor. Geophys.* **2002**, *33*, 90–94.

67. Cameron, D.R.; Dejong, E.; Read, D.W.L.; Oosterveld, M. Mapping Salinity Using Resistivity and Electromagnetic Inductive Techniques. *Can. J. Soil Sci.* **1981**, *61*, 67–78.

68. Bourgault, G.; Journel, A.G.; Rhoades, J.D.; Corwin, D.L.; Lesch, S.M. Geostatistical analysis of a soil salinity data set. *Adv. Agronomy* **1996**, *58*, 241–292.

69. De Clercq, W.; Rozanov, A. Using Iodine as a Tracer in the Field and the Detection Thereof to Reflect on Water and Salt Movement in These Soils. In Proceedings of the 3rd Global Workshop on Proximal Soil Sensing, Postdam, Germany, 26–29 May 2013; p. 252.

70. Fitzpatrick, R.W.; Thomas, M.; Davies, P.J.; Williams, B.G. *Dry Saline Land: An Investigation Using Ground-Based Geophysics, Soil Survey and Spatial Methods near Jamestown, South Australia*; CSIRO Land and Water: Glen Osmond, Australia, 2003.

71. Hendrickx, J.M.H.; Baerends, B.; Raza, Z.I.; Sadig, M.; Chaudhry, M.A. Soil-Salinity Assessment by Electromagnetic Induction of Irrigated Land. *Soil Sci. Soc. Am. J.* **1992**, *56*, 1933–1941.

72. Hopkins, D.G.; Richardson, J.L. Detecting a salinity plume in an unconfined sandy aquifer and assessing secondary soil salinization using electromagnetic induction techniques, North Dakota, USA. *Hydrogeol. J.* **1999**, *7*, 380–392.

73. Huang, J.; Subasinghe, R.; Malik, R.; Triantafilis, J. Salinity hazard and risk mapping of point source salinisation using proximally sensed electromagnetic instruments. *Comput. Electron. Agric.* **2015**, *113*, 213–224.

74. Huang, J.; Mokhtari, A.; Cohen, D.; Monteiro Santos, F.; Triantafilis, J. Modelling soil salinity across a gilgai landscape by inversion of EM38 and EM31 data. *Eur. J. Soil Sci.* **2015**, *66*, 951–960.

75. Lesch, S.M.; Rhoades, J.D.; Corwin, D.L. Statistical Modeling and Prediction Methodologies for Large Scale Spatial Sil Salinity Characterization: A Case Study Using Calibrated Electromagnetic Measurements Within the Broadview Water District. Available online: https://pdfs.semanticscholar.org/d741/83bae61378577de128283ea0139f9f0a73dc.pdf (accessed on 1 November 2017).

76. Lesch, S.M.; Strauss, D.J.; Rhoades, J.D. Spatial Prediction of Soil-Salinity Using Electromagnetic Induction Techniques 1. Statistical Prediction Models—A Comparison of Multiple Linear-Regression and Cokriging. *Water Resour. Res.* **1995**, *31*, 373–386.

77. Lesch, S.M.; Herrero, J.; Rhoades, J.D. Monitoring for temporal changes in soil salinity using electromagnetic induction techniques. *Soil Sci. Soc. Am. J.* **1998**, *62*, 232–242.

78. Mankin, K.R.; Ewing, K.L.; Schrock, M.D.; Kluitenberg, G.J. Field measurement and mapping of soil salinity in saline seeps. In Proceedings of the ASAE International Meeting; Minneapolis, MN, USA, 10–14 August 1997.

79. Mankin, K.; Koelliker, J. Hydrologic balance approach to saline seep remediation design. *Appl. Eng. Agric.* **2000**, *16*, 129–133.

80. Mankin, K.R.; Karthikeyan, R. Field assessment of saline seep remediation using electromagnetic induction. *Trans. ASAE* **2002**, *45*, 99–107.

81. Turnham, C. Using electromagnetic induction methods to measure just a Bullet Point agricultural soil salinity and its effects on adjacent native vegetation in Western Australia. BSc. Thesis, Lancaster University, 2003.

82. Lelij, A.V.D. *Use of an Electromagnetic Induction Measurement (Type EM-38) for Mapping of Soil Salinity*; Water Resource Commission: Murrumbidgee, Australia, 1983; p. 22.

83. Barr, N.F. Salinity Control, Water Reform and Structural Adjustment: The Tragowel Plains Irrigation District. Ph.D. Thesis, University of Melbourne, Melbourne, Australia, 1999.

84. Bennett, D.; George, R. Using the EM38 to measure the effect of soil salinity on Eucalyptus globulus in south-western Australia. *Agric. Water Manag.* **1995**, *27*, 69–85.

85. Bouksila, F.; Persson, M.; Bahri, A.; Berndtsson, R. Electromagnetic induction prediction of soil salinity and groundwater properties in a Tunisian Saharan oasis. *Hydrol. Sci. J.* **2012**, *57*, 1473–1486.

86. Slavich, P.; Johnston, S. Sources of acidity and pathways of transport to the Belongil drainage system. Available online: http://www.wetlandcare.com.au/Content/templates/..%5C..%5Cdocs%5Creports%5CBelongil%20Working%20Papers.pdf#page=10 (accessed on 1 November 2017).

87. Chaali, N.; Coppola, A.; Comegna, A.; Dragonetti, G. Assessment of Soil Electromagnetic Parameters and Their Variation with Soil Water, Salts: A Comparison among EMI and TDR Measuring Methods. In Proceedings of the EGU General Assembly Conference Abstracts, Vienna, Austria, 12–17 April 2015.

88. Corwin, D.L.; Lesch, S.M.; Shouse, P.J.; Soppe, R.; Ayars, J.E. Identifying soil properties that influence cotton yield using soil sampling directed by apparent soil electrical conductivity. *Agron. J.* **2003**, *95*, 352–364.

89. Smitt, C.; Cox, J.; McEwan, K.; Davies, P.; Herczeg, A.; Walker, G. *Salt Transport in the Bremer Hills, interpretation of Spatial Datasets for Salt Distribution*; Technical Report 49/03, CSIRO Land and Water: Canberra, Austrialia. Available online: http://www.clw.csiro.au/publications/technical2003/tr49-03.pdf (accessed on 1 November 2017).

90. Evans, T. Mapping vineyard salinity using electromagnetic surveys. *Aust. Grapegrow. Winemak.* **1998**, *415*, 20–21.

91. Hanson, B.R.; Kaita, K. Response of electromagnetic conductivity meter to soil salinity and soil-water content. *J. Irrig. Drain. Eng.—ASCE* **1997**, *123*, 141–143.

92. Horney, R.D.; Taylor, B.; Munk, D.S.; Roberts, B.A.; Lesch, S.M.; Plant, R.E. Development of practical site-specific management methods for reclaiming salt-affected soil. *Comput. Electron. Agric.* **2005**, *46*, 379–397.

93. Spies, B.; Woodgate, P. Salinity Mapping Methods in the Australian Context. Available online: https://www.researchgate.net/profile/Peter_Woodgate/publication/242771344_Salinity_mapping_methods_in_the_Australian_context/links/5418c99f0cf2218008bf4575.pdf (accessed on 1 November 2017).

94. Cannon, M.E.; McKenzie, R.C.; Lachapelle, G. Soil-Salinity Mapping with Electromagnetic Induction and Satellite-Based Navigation Methods. *Can. J. Soil Sci.* **1994**, *74*, 335–343.

95. Yao, R.; Yang, J. Quantitative evaluation of soil salinity and its spatial distribution using electromagnetic induction method. *Agric. Water Manag.* **2010**, *97*, 1961–1970.

96. Yao, Y.; Zhang, F.; Jiang, H. Research on model of soil salinization monitoring based on hyperspectral index and EM38. *Spectrosc. Spectr. Anal.* **2013**, *33*, 1658–1664.

97. Corwin, D.L.; Lesch, S.M. Application of Soil Electrical Conductivity to Precision Agriculture: Theory, Principles, and Guidelines. *Agron. J.* **2003**, *95*, 455–471.

98. Soliman, A.S. Detecting Salinity in Early Stages Using Electromagnetic Survey and Multivariate Geostatistical Technique: A Case Study of Nong Suang District, Nakhon Ratchasima, Thailand. Available online: https://www.semanticscholar.org/paper/Detecting-salinity-in-early-stages-using-electroma-Soliman/b7c1d14212dcd1ab4f55b473aad5489771d7c56d (accessed on 1 November 2017).

99. Norman, C.P.; Lyle, C.W.; Heuperman, A.F. Pyramid Hill Irrigation Area: Soil Salinity Survey May–June, 1988 (Victoria). Available online: http://agris.fao.org/agris-search/search.do?recordID=AU9430078 (accessed on 1 November 2017).

100. Lesch, S.M.; Corwin, D.L.; Robinson, D.A. Apparent soil electrical conductivity mapping as an agricultural management tool in arid zone soils. *Comput. Electron. Agric.* **2005**, *46*, 351–378.

101. Salama, R.; Bartle, G.; Farrington, P.; Wilson, V. Basin geomorphological controls on the mechanism of recharge and discharge and its effect on salt storage and mobilization—Comparative study using geophysical surveys. *J. Hydrol.* **1994**, *155*, 1–26.

102. Zhu, Q.; Lin, H.; Doolittle, J. Repeated Electromagnetic Induction Surveys for Improved Soil Mapping in an Agricultural Landscape. *Soil Sci. Soc. Am. J.* **2010**, *74*, 1763–1774.

103. Bobert, J.; Schmidt, F.; Gebbers, R.; Selige, T.; Schmidhalter, U. Estimating Soil Moisture Distribution for Crop Management with Capacitance Probes, EM-38 and Digital Terrain Analysis. In Proceedings of the 3rd European Conference on Precision Agriculture, Montpellier, France, 16–20 June 2001; pp. 349–359.

104. Vitharana, U.W.A.; Van Meirvenne, M.; Cockx, L.; Bourgeois, J. Identifying potential management zones in a layered soil using several sources of ancillary information. *Soil Use Manag.* **2006**, *22*, 405–413.

105. Lück, E.; Eisenreich, M.; Domsch, H.; Blumenstein, O. Geophysik für Landwirtschaft und Bodenkunde. In *Geophysik für Landwirtschaft und Bodenkunde*; Selbstverl. der Arbeitsgruppe Stoffdynamik in Geosystemen: Potsdam, Gemany; 2000.

106. Bang, J. Characterization of Soil Spatial Variability for Sitespecific Management Using Soil Electrical Conductivity and Other Remotely Sensed Data. Ph.D. Thesis, North Carolina State University, Raleigh, NC, USA, 2005.

107. Luck, E.; Gebbers, R.; Ruehlmann, J.; Spangenberg, U. Electrical conductivity mapping for precision farming. *Near Surf. Geophys.* **2009**, *7*, 15–25.

108. Heil, K.; Schmidhalter, U. Characterisation of soil texture variability using the apparent soil electrical conductivity at a highly variable site. *Comput. Geosci.—UK* **2012**, *39*, 98–110.

109. Mertens, F.M.; Paetzold, S.; Welp, G. Spatial heterogeneity of soil properties and its mapping with apparent electrical conductivity. *J. Plant Nutr. Soil Sci.* **2008**, *171*, 146–154.

110. Zhu, Q.; Lin, H.; Doolittle, J. Repeated electromagnetic induction surveys for determining subsurface hydrologic dynamics in an agricultural landscape. *Soil Sci. Soc. Am. J.* **2010**, *74*, 1750–1762.

111. Zhu, Q.; Lin, H. Comparing ordinary kriging and regression kriging for soil properties in contrasting landscapes. *Pedosphere* **2010**, *20*, 594–606.

112. Corwin, D.L.; Lesch, S.M. Characterizing soil spatial variability with apparent soil electrical conductivity: Part II. Case study. *Comput. Electron. Agric.* **2005**, *46*, 103–133.

113. McBratney, A.B.; Minasny, B.; Whelan, B.M. Obtaining 'Useful' High-Resolution Soil Data from Proximally-Sensed Electrical Conductivity/Resistivity (PSEC/R) Surveys. *Precis. Agric.* **2005**, *5*, 503–510.

114. Minasny, B.; McBratney, A.B. Estimating the water retention shape parameter from sand and clay content. *Soil Sci. Soc. Am. J.* **2007**, *71*, 1105–1110.

115. Waine, T.W.; Blackmore, B.S.; Godwin, R.J. Mapping available water content and estimating soil textural class using electro-magnetic induction. *Proc. EurAgEng* **2000**, *Paper 00-SW*, 44.

116. Domsch, H.; Giebel, A. Estimation of Soil Textural Features from Soil Electrical Conductivity Recorded Using the EM38. *Precis. Agric.* **2004**, *5*, 389–409.

117. Doolittle, J.A.; Indorante, S.J.; Potter, D.K.; Hefner, S.G.; McCauley, W.M. Comparing three geophysical tools for locating sand blows in alluvial soils of southeast Missouri. *J. Soil Water Conserv.* **2002**, *57*, 175–182.

118. Harvey, O.R.; Morgan, C.L.S. Predicting Regional-Scale Soil Variability using a Single Calibrated Apparent Soil Electrical Conductivity Model. *Soil Sci. Soc. Am. J.* **2009**, *73*, 164–169.

119. Triantafilis, J.; Lesch, S.M. Mapping clay content variation using electromagnetic induction techniques. *Comput. Electron. Agric.* **2005**, *46*, 203–237.

120. Kühn, J.; Brenning, A.; Wehrhan, M.; Koszinski, S.; Sommer, M. Interpretation of electrical conductivity patterns by soil properties and geological maps for precision agriculture. *Precis. Agric.* **2009**, *10*, 490–507.

121. Weller, U.; Zipprich, M.; Sommer, M.; Castell, W.Z.; Wehrhan, M. Mapping clay content across boundaries at the landscape scale with electromagnetic induction. *Soil Sci. Soc. Am. J.* **2007**, *71*, 1740–1747.

122. Schmidhalter, U.; Zintel, A. Schätzung der räumlichen Variationen des Ton- und Wassergehaltes mit elektromagnetischer Induktion. *Mitteilungen Deutschen Bodenkundlichen Gesellschaft* **1999**, *91*, 871–874.

123. Schmidhalter, U.A.; Zintel, A.; Neudecker, E. Calibration of Electromagnetic Induction Measurements to Survey the Spatial Variability of Soils. In Proceedings of the 3rd European Conference on Precision Agriculture, Montpellier, France, 18–20 June 2001; pp. 479–484.

124. Delin, S.; Soderstrom, M. Performance of soil electrical conductivity and different methods for mapping soil data from a small dataset. *Acta Agric. Scand. Sect. B—Soil Plant Sci.* **2003**, *52*, 127–135.

125. Korsaeth, A. Soil apparent electrical conductivity (ECa) as a means of monitoring changesin soil inorganic n on heterogeneous morainic soils in SE Norway during two growing seasons. *Nutr. Cycl. Agroecosyst.* **2005**, *72*, 213–227.

126. Korsaeth, A. Relations between electrical conductivity, soil texture and chemical properties on a clay soil in Southern Norway. DIAS Report, Plant Production No. 100; Apelsvoll Research Centre, The Norwegian Crop Research Institute: Kapp, Norway, September 2003; pp. 139–142.

127. Lukas, V.; Neudert, L.; Kren, J. Mapping of soil conditions in precision agriculture. *Acta Agrophys.* **2009**, *13*, 393–405.

128. Nehmdahl, H.; Greve, M.H. Using Soil Electrical Conductivity Measurements for Delineating Management Zones on Highly Variable Soils in Denmark. In Proceedings of the 3rd European Conference on Precision Agriculture, Montpellier, France, 18–20 June 2001; pp. 461–466.

129. Saey, T.; Van Meirvenne, M.; Vermeersch, H.; Ameloot, N.; Cockx, L. A pedotransfer function to evaluate the soil profile textural heterogeneity using proximally sensed apparent electrical conductivity. *Geoderma* **2009**, *150*, 389–395.

130. Corwin, D.L.; Kaffka, S.R.; Hopmans, J.W.; Mori, Y.; van Groenigen, J.W.; van Kessel, C.; Lesch, S.M.; Oster, J.D. Assessment and field-scale mapping of soil quality properties of a saline-sodic soil. *Geoderma* **2003**, *114*, 231–259.

131. Grigera, M.S.; Drijber, R.A.; Eskridge, K.M.; Wienhold, B.J. Soil microbial biomass relationships with organic matter fractions in a Nebraska corn field mapped using apparent electrical conductivity. *Soil Sci. Soc. Am. J.* **2006**, *70*, 1480–1488.

132. Jung, W.K.; Kitchen, N.R.; Sudduth, K.A.; Kremer, R.J.; Motavalli, P.P. Relationship of apparent soil electrical conductivity to claypan soil properties. *Soil Sci. Soc. Am. J.* **2005**, *69*, 883–892.

133. Sudduth, K.A.; Kitchen, N.R. Mapping Soil Electrical Conductivity. *Remote Sens. Agric. Environ.* **2004**, 188–201.

134. Triantafilis, J.; Odeh, I.O.A.; McBratney, A.B. Five geostatistical models to predict soil salinity from electromagnetic induction data across irrigated cotton. *Soil Sci. Soc. Am. J.* **2001**, *65*, 869–878.

135. Hedley, C.B.; Yule, I.Y.; Eastwood, C.R.; Shepherd, T.G.; Arnold, G. Rapid identification of soil textural and management zones using electromagnetic induction sensing of soils. *Aust. J. Soil Res.* **2004**, *42*, 389–400.

136. Van Meirvenne, M.; Verdoodt, A.; Lenoir, H.; Saey, T.; Haputanthri, T. Response of EMI based proximal soil sensor in two contrasting tropical landscapes. In Proceedings of the 3rd Global Workshop on Proximal Soil Sensing, Postdam, Germany, 26–29 May 2013; p. 56.

137. Dalgaard, M.; Have, H.; Nehmdahl, H. Soil clay mapping by measurement of electromagnetic conductivity. In Proceedings of the 3rd European Conference on Precision Agriculture, Montpellier, France, 18–20 June 2001; pp. 367–372.

138. Brevik, E.C.; Fenton, T.E. Influence of soil water content, clay, temperature, and carbonate minerals on electrical conductivity readings taken with an EM-38. *Soil Horiz.* **2002**, *43*, 9–13.

139. Brevik, E.C.; Fenton, T.E.; Lazari, A. Soil electrical conductivity as a function of soil water content and implications for soil mapping. *Precis. Agric.* **2006**, *7*, 393–404.

140. Hedley, C.; Roudier, P.; Yule, I.; Ekanayake, J.; Bradbury, S. Soil water status and water table depth modelling using electromagnetic surveys for precision irrigation scheduling. *Geoderma* **2013**, *199*, 22–29.

141. Kachanoski, R.; Wesenbeeck, I.V.; Gregorich, E. Estimating spatial variations of soil water content using noncontacting electromagnetic inductive methods. *Can. J. Soil Sci.* **1988**, *68*, 715–722.

142. Kachanoski, R.; Wesenbeeck, I.V.; Jong, E.D. Field scale patterns of soil water storage from non-contacting measurements of bulk electrical conductivity. *Can. J. Soil Sci.* **1990**, *70*, 537–542.

143. Khakural, B.R.; Robert, P.C.; Hugins, D.R. Use of non-contacting electromagnetic inductive method for estimating soil moisture across a landscape. *Commun. Soil Sci. Plant Anal.* **1998**, *29*, 2055–2065.

144. Kravchenko, A.; Bollero, G.; Omonode, R.; Bullock, D. Quantitative mapping of soil drainage classes using topographical data and soil electrical conductivity. *Soil Sci. Soc. Am. J.* **2002**, *66*, 235–243.

145. Malo, D.D.; Lee, D.K.; Lee, J.H.; Christopherson, C.M. Soil Mositure, Bulk Densityy, Soil Temperature, and Soil Sensor (Veris 3100® and Geonics Em-38®) Relationships: Part1—Moody County Site. Progress report. South Dakota State University: Brookings, SD, USA, 2001.

146. Jiang, P.; Anderson, S.H.; Kitchen, N.R.; Sudduth, K.A.; Sadler, E.J. Estimating plant-available water capacity for claypan landscapes using apparent electrical conductivity. *Soil Sci. Soc. Am. J.* **2007**, *71*, 1902–1908.

147. Morgan, C.; Norman, J.; Wolkowski, R.; Lowery, B.; Morgan, G.; Schuler, R. Two Approaches to Mapping Plant Available Water: EM-38 Measurements and Inverse Yield Modeling. In Proceedings of the 5th International Conference on Precision Agriculture, Bloomington, MI, USA, 16–19 July 2000; pp. 1–13.

148. Reedy, R.C.; Scanlon, B.R. Soil Water Content Monitoring Using Electromagnetic Induction. *J. Geotech. Geoenviron. Eng.* **2003**, *129*, 1028–1039.

149. Reedy, R.C.; Scanlon, B.R. Assessing the Impact of Land Use on Groundwater Recharge in the Southern High Plains. In Proceedings of the 2003 AGU Fall Meeting Abstracts, San Francisco, CA, USA.

150. Sheets, K.R.; Hendrickx, J.M.H. Noninvasive Soil Water Content Measurement Using Electromagnetic Induction. *Water Resour. Res.* **1995**, *31*, 2401–2409.

151. Erindi-kati, A. Remote Sensing and Root Zone Soil Moisture. McGill University, Montreal, QC, Canada, 2005.

152. Wong, M.T.F.; Asseng, S. Determining the causes of spatial and temporal variability of wheat yields at sub-field scale using a new method of upscaling a crop model. *Plant Soil* **2006**, *283*, 203–215.

153. Misra, R.K.; Padhi, J. Assessing field-scale soil water distribution with electromagnetic induction method. *J. Hydrol.* **2014**, *516*, 200–209.

154. De Benedetto, D.; Castrignanò, A.; Rinaldi, M.; Ruggieri, S.; Santoro, F.; Figorito, B.; Gualano, S.; Diacono, M.; Tamborrino, R. An approach for delineating homogeneous zones by using multi-sensor data. *Geoderma* **2013**, *199*, 117–127.

155. Malo, D.D.; Lee, D.K.; Lee, J.H.; Christopherson, S.M.; Cole, C.M.; Kleinjan, J.L.; Carlson, C.G.; Clay, D.E.; Chang, J.; Reese, C.L.; et al. Soil Moisture, Bulk Density, Soil Temperature, and Soil Sensor (Veris 3100® And Geonics EM-38®) Moody County Site. Annual Report Soil PR00-41; South Dakota State Univertisy: Brookings, SD, USA, 2000.

156. Buchanan, S.; Triantafilis, J. Mapping Water Table Depth Using Geophysical and Environmental Variables. *Ground Water* **2009**, *47*, 80–96.

157. Doolittle, J.; Noble, C.; Leinard, B. An electromagnetic induction survey of a riparian area in southwest Montana. *Soil Horiz.* **2000**, *41*, 27–36.

158. Fenton, T.E.; Lauterbach, M.A. Soil Map Unit Composition and Scale of Mapping Related to Interpretations for Precision Soil and Crop Management in Iowa. In Proceedings of the 4th International Conference on Precision Agriculture, St. Paul, MN, USA, 19–22 July 1998.

159. Hall, L.M.; Brainard, J.R.; Bowman, R.S.; Hendrickx, J.M.H. Determination of solute distributions in the vadose zone using downhole electromagnetic induction. *Vadose Zone J.* **2004**, *3*, 1207–1214.

160. Schumann, A.; Zaman, Q. Mapping water table depth by electromagnetic induction. *Appl. Eng. Agric.* **2003**, *19*, 675–688.

161. Wilson, R.C.; Freeland, R.S.; Wilkerson, J.B.; Yoder, R.E. Imaging the Lateral Migration of Subsurface Moisture using Electromagnetic Induction; In Proceedings of the American Society of Agricultural and Biological Engineers Annual International Meeting, Chicago, IL, USA, 28–31 July 2002; p. 16.

162. Wilson, R.C.; Freeland, R.S.; Wilkerson, J.B.; Yoder, R.E. Inferring subsurface morphology from transient soil moisture patterns using electrical conductivity. *Trans. ASAE* **2003**, *46*, 1435–1441.

163. Vervoort, R.W.; Annen, Y.L. Palaeochannels in Northern New South Wales: Inversion of electromagnetic induction data to infer hydrologically relevant stratigraphy. *Aust. J. Soil Res.* **2006**, *44*, 35–45.

164. Rhoades, J.D.; Lesch, S.M.; LeMert, R.D.; Alves, W.J. Assessing irrigation/drainage/salinity management using spatially referenced salinity measurements. *Agric. Water Manag.* **1997**, *35*, 147–165.

165. Hedley, C.; Yule, I. Soil water status mapping and two variable-rate irrigation scenarios. *Precis. Agric.* **2009**, *10*, 342–355.

166. Weaver, T.; Hulugalle, N.; Ghadiri, H. Estimating drainage under cotton with chloride mass balance and an EM38. *Commun. Soil Sci. Plant Anal.* **2013**, *44*, 1700–1707.

167. Corwin, D.L.; Lesch, S.M. Characterizing soil spatial variability with apparent soil electrical conductivity I. Survey protocols. *Comput. Electron. Agric.* **2005**, *46*, 103–133.

168. Saey, T.; Simpson, D.; Vermeersch, H.; Cockx, L.; Van Meirvenne, M. Comparing the EM38DD and DUALEM-21S Sensors for Depth-to-Clay Mapping. *Soil Sci. Soc. Am. J.* **2009**, *73*, 7–12.

169. Sherlock, M.D.; McDonnell, J.J. A new tool for hillslope hydrologists: Spatially distributed groundwater level and soilwater content measured using electromagnetic induction. *Hydrol. Process.* **2003**, *17*, 1965–1977.

170. Cook, S.; Adams, M.; Corner, R. On-farm experimentation to determine site-specific responses to variable inputs. *Precis. Agric.* **1999**, 611–621.

171. Ammons, J.T.; Timpson, M.E.; Newton, D.L. Application of aboveground electromagnetic conductivity meter to separate Natraqalfs and Ochraqualfs in Gibson County. *Soil Surv. Horiz.* **1989**, *30*, 66–70.

172. Anderson-Cook, C.M.; Alley, M.; Roygard, J.; Khosla, R.; Noble, R.; Doolittle, J. Differentiating soil types using electromagnetic conductivity and crop yield maps. *Soil Sci. Soc. Am. J.* **2002**, *66*, 1562–1570.

173. Brevik, E.C.; Fenton, T.E.; Jaynes, D.B. The use of soil electrical conductivity to investigate soil homogeneity in Story County, Iowa, USA. *Soil Horiz.* **2012**, *53*, 50–54.

174. Dampney, P.; King, J.; Lark, R.; Wheeler, H.; Bradley, R.; Mayr, T. Automated methods for mapping patterns of soil physical properties as a basis for variable management of crops within fields. In *Precision Agriculture*; Stafford, J., Werner, A., Eds; Wageningen Academic Publishers: Wageningen, The Netherlands, 2003; pp. 135–140.

175. Greve, M.B.; Greve, M.H. Decision Support System for Classification and Representation of Fuzzy Soil Boundaries. In Proceedings of the 19th European and Scandinavian Conference for ESRI Users, Copenhagen, Denmark, 8–10 November 2004.

176. Hinck, S.; Mueller, K.; Emeis, N. Part Field Management: Comparison of EC-value, soil texture, nutrient content and biomass in two selected fields. In Proceedings of the 3rd Global Workshop on Proximal Soil Sensing, Postdam, Germany, 26–29 May 2013; p. 270.

177. Huang, J.; Nhan, T.; Wong, V.N.L.; Johnston, S.G.; Lark, R.M.; Triantafilis, J. Digital soil mapping of a coastal acid sulfate soil landscape. *Soil Res.* **2014**, *52*, 327–339.

178. James, I.T.; Waine, T.W.; Bradley, R.I.; Taylor, J.C.; Godwin, R.J. Determination of soil type boundaries using electromagnetic induction scanning techniques. *Biosyst. Eng.* **2003**, *86*, 421–430.

179. Rampant, P.; Abuzar, M. Geophysical Tools and Digital Elevation Models: Tools for Understanding Crop Yield and Soil Variability. In Proceedings of the SuperSoil 2004—3rd Australian New Zealand Soils Conference,Sydney, Australia, 5–9 December 2004.

180. Triantafilis, J. Hydrostratigraphic Analysis Using Electromagnetic Induction Data and a Quasi-Three-Dimensional Electrical Conductivity Imaging. In Proceedings of the 3rd Global Workshop on Proximal Soil Sensing, Potsdam, Gemany, 26–29 May 2013; pp. 34–38.

181. Stroh, J.C.; Archer, S.; Doolittle, J.A.; Wilding, L. Detection of edaphic discontinuities with ground-penetrating radar and electromagnetic induction. *Landsc. Ecol.* **2001**, *16*, 377–390.

182. Bönecke, E.; Franko, U. A Modelling Approach to Find Stable and Reliable Soil Organic Carbon Values for Further Regionalization. In Proceedings of the EGU General Assembly Conference Abstracts, Vienna, Austria, 12–17 April 2015.

183. Doolittle, J.A.; Collins, M.E. A comparison of EM induction and GPR methods in areas of karst. *Geoderma* **1998**, *85*, 83–102.

184. Doolittle, J.A.; Sudduth, K.A.; Kitchen, N.R.; Indorante, S.J. Estimating Depths to Claypans Using Electromagnetic Induction Methods. *J. Soil Water Conserv.* **1994**, *49*, 572–575.

185. Gebbers, R.; Lück, E.; Heil, K. Depth sounding with the EM38-detection of soil layering by inversion of apparent electrical conductivity measurements. *Precis. Agric.* **2007**, *7*, 95–102.

186. Kimble, J.M.; Doolittle, J.; Taylor, R.; Windhorn, R.; Gerken, J. The Use of EMI and Electrical Instruments for Estimating Soil Properties to Help in Mapping. In Proceedings of the 2001 AGU Fall Meeting Abstract, San Francisco, CA, USA, 10–14 December 2001.

187. Kitchen, N.R.; Sudduth, K.A.; Drummond, S.T. Mapping of sand deposition from 1993 midwest floods with electromagnetic induction measurements. *J. Soil Water Conserv.* **1996**, *51*, 336–340.

188. Knotters, M.; Brus, D.J.; Voshaar, J.H.O. A Comparison of Kriging, Co-Kriging and Kriging Combined with Regression for Spatial Interpolation of Horizon Depth with Censored Observations. *Geoderma* **1995**, *67*, 227–246.

189. Vitharana, U.W.A.; Saey, T.; Cockx, L.; Simpson, D.; Vermeersch, H.; Van Meirvenne, M. Upgrading a 1/20,000 soil map with an apparent electrical conductivity survey. *Geoderma* **2008**, *148*, 107–112.

190. Boettinger, J.; Doolittle, J.; West, N.; Bork, E.; Schupp, E.W. Nondestructive assessment of rangeland soil depth to petrocalcic horizon using electromagnetic induction. *Arid Land Res. Manag.* **1997**, *11*, 375–390.

191. Bork, E.W.; West, N.E.; Doolittle, J.A.; Boettinger, J.L. Soil depth assessment of sagebrush grazing treatments using electromagnetic induction. *J. Range Manag.* **1998**, *51*, 469–474.

192. Brevik, E.; Fenton, T.; Horton, R. Effect of Daily Soil Temperature Fluctuations on Soil Electrical Conductivity as Measured with the Geonics® EM-38. *Precis. Agric.* **2004**, *5*, 145–152.

193. Brus, D.J.; Knotters, M.; Vandooremolen, W.A.; Vankernebeek, P.; Vanseeters, R.J.M. The Use of Electromagnetic Measurements of Apparent Soil Electrical-Conductivity to Predict the Boulder Clay Depth. *Geoderma* **1992**, *55*, 79–93.

194. Cai, C.; Lin, J.; Meng, F.; Sun, Y.; Li, D. Estimation of topsoil thickness in reclaimed field using EM38. *Trans. Chin. Soc. Agric. Eng.* **2010**, *26*, 319–323.

195. Grellier, S.; Florsch, N.; Camerlynck, C.; Janeau, J.L.; Podwojewski, P.; Lorentz, S. The use of Slingram EM38 data for topsoil and subsoil geoelectrical characterization with a Bayesian inversion. *Geoderma* **2013**, *200*, 140–155.

196. Sudduth, K.A.; Kitchen, N.R.; Hughes, D.F.; Drummond, S.T. Electromagnetic Induction Sensing as an Indicator of Productivity on Claypan Soils. In *Site-Specific Management for Agricultural Systems*; American Society of Agronomy, Crop Science Society of America, Soil Science Society of America: Madison, WI, USA, 1995; pp. 671–681.

197. Sudduth, K.A.; Kitchen, N.R.; Bollero, G.A.; Bullock, D.G.; Wiebold, W.J. Comparison of electromagnetic induction and direct sensing of soil electrical conductivity. *Agron. J.* **2003**, *95*, 472–482.

198. Sudduth, K.; Kitchen, N. Electromagnetic Induction Sensing of Claypan Depth. *Am. Soc. Agric. Eng.* **1993**.

199. Corwin, D.L. Delineating Site-Specific Crop Management Units: Precision Agriculture Application in GIS. In Proceedings of the 2005 ESRI International Users Conference, San Diego, CA, USA, 25–29 July 2005.

200. Triantafilis, J.; Santos, F.M. 2-dimensional soil and vadose-zone representation using an EM38 and EM34 and a laterally constrained inversion model. *Soil Res.* **2010**, *47*, 809–820.

201. McBride, R.A.; Gordon, A.M.; Shrive, S.C. Estimating Forest Soil Quality from Terrain Measurements of Apparent Electrical-Conductivity. *Soil Sci. Soc. Am. J.* **1990**, *54*, 290–293.

202. Lück, E. Conductivity Mapping to Characterize the Spatial Variability within Large Fields. In Proceedings of the 6th International Conference on Precision Agriculture and Other Precision Resources Management, Minneapolis, MN, USA, 14–17 July 2002.

203. Martinez, G.; Vanderlinden, K.; Ordóñez, R.; Muriel, J.L. Can Apparent Electrical Conductivity Improve the Spatial Characterization of Soil Organic Carbon? All rights reserved. No part of this periodical may be reproduced or transmitted in any form or by any means, electronic or mechanical, including photocopying, recording, or any information storage and retrieval system, without permission in writing from the publisher. *Vadose Zone J.* **2009**, *8*, 586–593.

204. Johnson, C.K.; Eskridge, K.M.; Corwin, D.L. Apparent soil electrical conductivity: Applications for designing and evaluating field-scale experiments. *Comput. Electron. Agric.* **2005**, *46*, 181–202.

205. Islam, M.M.; Saey, T.; De Smedt, P.; Van De Vijver, E.; Delefortrie, S.; Van Meirvenne, M. Modeling within field variation of the compaction layer in a paddy rice field using a proximal soil sensing system. *Soil Use Manag.* **2014**, *30*, 99–108.

206. Islam, M.M.; Meerschman, E.; Saey, T.; De Smedt, P.; Van De Vijver, E.; Delefortrie, S.; Van Meirvenne, M. Characterizing compaction variability with an electromagnetic induction sensor in a puddled paddy rice field. *Soil Sci. Soc. Am. J.* **2014**, *78*, 579–588.

207. Jung, W.K.; Kitchen, N.R.; Sudduth, K.A.; Anderson, S.H. Spatial characteristics of claypan soil properties in an agricultural field. *Soil Sci. Soc. Am. J.* **2006**, *70*, 1387–1397.

208. Krajco, J. Detection of Soil Compaction Using Soil Electrical Conductivity. MSc. Thesis. Cranfield University: Cranfield, UK, 2007. Available online: https://dspace.lib.cranfield.ac.uk/bitstream/1826/2346/2/MSc%20Thesis%20final.pdf (accessed on 1 November 2017).

209. Slavich, P.G.; Yang, J. Estimation of Field Scale Leaching Rates from Chloride Mass Balance and Electromagnetic Induction Measurements. *Irrig. Sci.* **1990**, *11*, 7–14.

210. Tarr, A.B.; Moore, K.J.; Bullock, D.G.; Dixon, P.M.; Burras, C.L. Improving Map Accuracy of Soil Variables Using Soil Electrical Conductivity as a Covariate. *Precis. Agric.* **2005**, *6*, 255–270.

211. Vasic, D.; Ambrus, D.; Bilas, V. Simple Linear Inversion of Soil Electromagnetic Properties from Analytical Model of Electromagnetic Induction Sensor. In Proceeding of the 2014 IEEE Sensors Applications Symposium (SAS), Queenstown, New Zealand, 18–20 February 2014; pp. 15–19.

212. Hendrickx, J.M.H.; Borchers, B.; Corwin, D.L.; Lesch, S.M.; Hilgendorf, A.C.; Schlue, J. Inversion of soil conductivity profiles from electromagnetic induction measurements: Theory and experimental verification. *Soil Sci. Soc. Am. J.* **2002**, *66*, 673–685.

213. Kitchen, N.; Sudduth, K.; Drummond, S. Soil electrical conductivity as a crop productivity measure for claypan soils. *J. Prod. Agric.* **1999**, *12*, 607–617.

214. Noellsch, A.J. Optimizing Crop N Use Efficiency Using Polymer-Coated Urea and Other N Fertilizer Sources Across Landscapes with Claypan Soils. MSc. Thesis, University of Missouri, Columbia, MS, USA, 2008.

215. Eigenberg, R.A.; Nienaber, J.A. Electromagnetic survey of cornfield with repeated manure applications. *J. Environ. Qual.* **1998**, *27*, 1511–1515.

216. Eigenberg, R.A.; Nienaber, J.A. Identification of Nutrient Distribution at Abandoned Livestock Manure Handling Site Using Electromagnetic Induction. In Proceedings of the 2001 American Society of Agricultural and Biological Engineers Annual Meeting, Sacramento, CA, USA, 30 July–1 August 2001.

217. Eigenberg, R.; Korthals, R.; Nienaber, J. Geophysical electromagnetic survey methods applied to agricultural waste sites. *J. Environ. Qual.* **1998**, *27*, 215–219.

218. Eigenberg, R.A.; Doran, J.W.; Nienaber, J.A.; Ferguson, R.B.; Woodbury, B.L. Electrical conductivity monitoring of soil condition and available N with animal manure and a cover crop. *Agric. Ecosyst. Environ.* **2002**, *88*, 183–193.

219. Eigenberg, R.A.; Nienaber, J.A. Electromagnetic induction methods applied to an abandoned manure handling site to determine nutrient buildup. *J. Environ. Qual.* **2003**, *32*, 1837–1843.

220. Eigenberg, R.; Nienaber, J. Soil conductivity map differences for monitoring temporal changes in an agronomic field. *Am. Soc. Agric. Eng. Pap.* **1999**, 993173.

221. Eigenberg, R.A.; Nienaber, J.A.; Woodbury, B.L.; Ferguson, R.B. Soil conductivity as a measure of soil and crop status—A four-year summary. *Soil Sci. Soc. Am. J.* **2006**, *70*, 1600–1611.

222. Stevens, R.; O'bric, C.; Carton, O. Estimating nutrient content of animal slurries using electrical conductivity. *J. Agric. Sci.* **1995**, *125*, 233–238.

223. Doran, J.W.; Parkin, T.B. Quantitative indicators of soil quality: A minimum data set. *Soil Sci. Soc. Am.* **1996**.

224. Fritz, R.; Malo, D.; Schumacher, T.; Clay, D.; Carlson, C.; Ellsbury, M.; Dalsted, K. Field comparison of two soil electrical conductivity measurement systems. *Precis. Agric.* **1999**, 1211–1217.

225. Ponitka, J.; Pößneck, J. Untersuchungen zur Teilflächenbewirtschaftung: Untersuchungen zur Anwendung ausgewählter teilflächenspezifischer Bewirtschaftungsmethoden am Beispiel eines Auenstandortes der Elbe. Available online: http://www.qucosa.de/fileadmin/data/qucosa/documents/1847/1165589915791-5456.pdf (accessed on 1 November 2017).

226. Jaynes, D.B.; Colvin, T.S.; Ambuel, J. Yield mapping by electromagnetic induction. In *Site-Specific Management for Agricultural Systems*; American Society of Agronomy, Crop Science Society of America, Soil Science Society of America: Madison, WI, USA, 1995; pp. 383–394.

227. Delin, S.; Lindén, B. Variations in Net Nitrogen Mineralisation within an Arable Field. *Acta Agric. Scand. Section B Soil Plant Sci.* **2002**, *52*, 78–85.

228. Dunn, B.W.; Beecher, H.G. Using electro-magnetic induction technology to identify sampling sites for soil acidity assessment and to determine spatial variability of soil acidity in rice fields. *Aust. J. Exp. Agric.* **2007**, *47*, 208–214.

229. Heiniger, R.W.; McBride, R.G.; Clay, D.E. Using soil electrical conductivity to improve nutrient management. *Agron. J.* **2003**, *95*, 508–519.

230. Nadler, A. Estimating the soil water dependence of the electrical conductivity soil solution/electrical conductivity bulk soil ratio. *Soil Sci. Soc. Am. J.* **1982**, *46*, 722–726.

231. Lund, E.D.; Christy, C.D.; Drummond, P.E. Practical applications of soil electrical conductivity mapping. Available online: http://citeseerx.ist.psu.edu/viewdoc/download?doi=10.1.1.512.2890&rep=rep1&type=pdf (accessed on 1 November 2017).

232. Heiniger, R.W.; Carl, C. Side-by-Side Comparisons of Uniform and Site-Specific Nutrient Applications. In *Precision Agriculture*; 1999; pp. 967–967.

233. Motavalli, P.P.; Hammer, R.D.; Bardhan, S. Apparent soil electrical conductivity used to determine soil phosphorus variability in poultry litter-amended pastures. *Yale Rev. Educ. Sci.* **2015**, 287–309.

234. Bekele, A.; Hudnall, W.H.; Daigle, J.J.; Prudente, J.A.; Wolcott, M. Scale dependent variability of soil electrical conductivity by indirect measures of soil properties. *J. Terramech.* **2005**, *42*, 339–351.

235. Zimmermann, H.M.; Plöchl, M.; Luckhaus, C.; Domsch, H. Selecting the optimum locations for soil investigations. *Precis. Agric.* **2003**; 759–764.

236. Lesch, S.M. Sensor-directed response surface sampling designs for characterizing spatial variation in soil properties. *Comput. Electron. Agric.* **2005**, *46*, 153–179.

237. Corwin, D.; Lesch, S.; Segal, E.; Skaggs, T.; Bradford, S. Comparison of Sampling Strategies for Characterizing Spatial Variability with Apparent Soil Electrical Conductivity Directed Soil Sampling. *J. Environ. Eng. Geophys.* **2010**, *15*, 147–162.

238. Heilig, J.; Kempenich, J.; Doolittle, J.; Brevik, E.C.; Ulmer, M. Evaluation of electromagnetic induction to characterize and map sodium-affected soils in the Northern Great Plains. *Soil Horiz.* **2011**, *52*, 77–88.

239. Johnson, C.K.; Doran, J.W.; Duke, H.R.; Wienhold, B.J.; Eskridge, K.M.; Shanahan, J.F. Field-scale electrical conductivity mapping for delineating soil condition. *Soil Sci. Soc. Am. J.* **2001**, *65*, 1829–1837.

240. Lesch, S.M.; Strauss, D.J.; Rhoades, J.D. Spatial Prediction of Soil-Salinity Using Electromagnetic Induction Techniques 2. An Efficient Spatial Sampling Algorithm Suitable for Multiple Linear-Regression Model Identification and Estimation. *Water Resour. Res.* **1995**, *31*, 387–398.

241. Lesch, S.; Rhoades, J.; Corwin, D. ESAP-95 version 2.01 R: User manual and tutorial guide. *Res. Rep.* **2000**, *146*, 17.

242. Yao, R.; Yang, J.; Zhao, X.; Chen, X.; Han, J.; Li, X.; Liu, M.; Shao, H. A New Soil Sampling Design in Coastal Saline Region Using EM38 and VQT Method. *Clean—Soil Air Water* **2012**, *40*, 972–979.

243. Shaner, D.L.; Khosla, R.; Brodahl, M.K.; Buchleiter, G.W.; Farahani, H.J. How well does zone sampling based on soil electrical conductivity maps represent soil variability? *Agron. J.* **2008**, *100*, 1472–1480.

244. Box, G.E.; Draper, N.R. *Empirical Model-Building and Response Surfaces*; Wiley: New York, NY, USA, 1987; Volume 424.

245. Tarr, A.B.; Moore, K.J.; Dixon, P.M.; Burras, C.L.; Wiedenhoeft, M.H. Use of soil electroconductivity in a multistage soil-sampling scheme. *Crop Manag.* **2003**, *2*.

246. Minasny, B.; McBratney, A.B. A conditioned Latin hypercube method for sampling in the presence of ancillary information. *Comput. Geosci.* **2006**, *32*, 1378–1388.

247. Niedzwiecki, J.D.G.; Pudelko, R. Electrical conductivity analysis of field of highly variable soils. In Proceedings of the 3rd Global Workshop on Proximal Soil Sensing, Potsdam, Germany, 26–29 May 2013.

248. Clay, D.E.; Chang, J.; Malo, D.D.; Carlson, C.G.; Reese, C.; Clay, S.A.; Ellsbury, M.; Berg, B. Factors influencing spatial variability of soil apparent electrical conductivity. *Commun. Soil Sci. Plant Anal.* **2001**, *32*, 2993–3008.

249. Neudecker, E.; Schmidhalter, U.; Sperl, C.; Selige, T. Site-Specific Soil Mapping by Electromagnetic Induction. In Proceedings of the 3rd European Conference on Precision Agriculture, Montpellier, France, 16–20 June 2001; pp. 271–276.

250. Bramley, R.G.V.; Trought, M.C.T.; Praat, J.P. Vineyard variability in Marlborough, New Zealand: characterising variation in vineyard performance and options for the implementation of Precision Viticulture. *Aust. J. Grape Wine Res.* **2011**, *17*, 72–78.

251. Bramley, R.G.V. Precision Viticulture—Tools to Optimise Winegrape Production in a Difficult Landscape. In Proceedings of the 6th International Conference on Precision Agriculture and Other Precision Resources Management, Minneapolis, MN, USA, 14–17 July 2002; p. 33.

252. Chang, J.Y.; Clay, D.E.; Carlson, C.G.; Clay, S.A.; Malo, D.D.; Berg, R.; Kleinjan, J.; Wiebold, W. Different techniques to identify management zones impact nitrogen and phosphorus sampling variability. *Agron. J.* **2003**, *95*, 1550–1559.

253. Cockx, L.; Meirvenne, M.V.; Hofman, G. The Use of Electromagnetic Induction in Delineating Nitrogen Management Zones. In Proceedings of the 7th International Conference on Precision Agriculture and Other Precision Resources Management, Minneapolis, MN, USA, 25–28 July 2004.

254. Cockx, L.; Van Meirvenne, M.; Hofman, G. Characterization of nitrogen dynamics in a pasture soil by electromagnetic induction. *Biol. Fertil. Soils* **2005**, *42*, 24–30.

255. Corwin, D. Past, present and future trends of soil soil electrical conductivity measurement using geophysical methods. In *Handbook of Agricultural Geophysics*; CRC Press: Boca Raton, FL, USA, 2008, pp. 17–44.

256. Delin, S. Site-specific Nitrogen Fertilization Demand in Relation to Plant Available Soil Nitrogen and Water. Available online: https://pub.epsilon.slu.se/730/ (accessed on 1 November 2017).

257. Domsch, H.; Kaiser, T.; Witzke, K.; Zauer, O. Empirical methods to detect management zones with respect to yield. *Precis. Agric.* **2003**, 187–192.

258. Fleming, K.L.; Westfall, D.G.; Bausch, W.C. Evaluating Management Zone Technology and Grid Soil Sampling for Variable Rate Nitrogen Application. In Proceedings of the 5th International Conference on Precision Agriculture, Bloomington, Minnesota, USA, 16–19 July 2000; p. 179.

259. Fountas, S.; Anastasiou, E.; Xanthopoulos, G.; Lambrinos, G.; Manolopoulou, E.; Apostolidou, S.; Lentzou, D.; Tsiropoulos, Z.; Balafoutis, A. Precision agriculture in watermelons. In *Precision Agriculture'15*; Wageningen Academic Publishers: Wageningen, The Netherlands, 2015; pp. 399–403.

260. Fraisse, C.W.; Sudduth, K.A.; Kitchen, N.R. Delineation of site-specific management zones by unsupervised classification of topographic attributes and soil electrical conductivity. *Trans. ASAE* **2001**, *44*, 155–166.

261. Franzen, D.; Kitchen, N. *Developing Management Zones to Target Nitrogen Applications*; Potash & Phosphate Institute: Atlanta, GA, USA, 1999.

262. Fridgen, J.J.; Kitchen, N.R.; Sudduth, K.A.; Drummond, S.T.; Wiebold, W.J.; Fraisse, C.W. Management Zone Analyst (MZA): Software for subfield management zone delineation. *Agron. J.* **2004**, *96*, 100–108.

263. Guretzky, J.A.; Moore, K.J.; Burras, C.L.; Brummer, E.C. Distribution of legumes along gradients of slope and soil electrical conductivity in pastures. *Agron. J.* **2004**, *96*, 547–555.

264. Islam, M.M.; Saey, T.; Meerschman, E.; De Smedt, P.; Meeuws, F.; Van De Vijver, E.; Van Meirvenne, M. Delineating water management zones in a paddy rice field using a Floating Soil Sensing System. *Agric. Water Manag.* **2011**, *102*, 8–12.

265. Islam, M.; Cockx, L.; Meerschman, E.; De Smedt, P.; Meeuws, F.; Van Meirvenne, M. A floating sensing system to evaluate soil and crop variability within flooded paddy rice fields. *Precis. Agric.* **2011**, *12*, 850–859.

266. Jaynes, D.; Colvin, T.; Ambuel, J. Soil Type and Crop Yield Determination from Ground Conductivity Surveys. *Am. Soc. Agric. Eng.* 1993.

267. Jaynes, D.B.; Colvin, T.S.; Kaspar, T.C. Identifying potential soybean management zones from multi-year yield data. *Comp. Electron. Agric.* **2005**, *46*, 309–327.

268. Kern, A.; Brevik, E.C.; Fenton, T.E.; Vincent, P.C. Comparisons of soil ECa maps to an order 1 soil survey for a Central Iowa field. *Soil Horiz.* **2008**, *49*, 36–39.

269. Kilborn, D.A.; Moore, K.J.; Hintz, R.L.; Tarr, A.B. Chariton Valley Biomass Project Task 5.10.0. Available online: http://www.iowaswitchgrass.com/__docs/pdf/5-10-0%20final%20report.pdf (accessed on 1 November 2017).

270. Lamb, D.; Bramley, R.; Hall, A. Precision Viticulture-an Australian Perspective. In Proceedings of the XXVI International Horticultural Congress: Viticulture-Living with Limitations 640, Toronto, ON, Canada, 11–17 August 2002; pp. 15–25.

271. Luchiari, A., Jr.; Shanahan, J.; Francis, D.; Schlemmer, M.; Schepers, J.; Liebig, M.; Schepers, A.; Payton, S. Strategies for Establishing Management Zones for Site Specific Nutrient Management. In Proceedings of the 5th International Conference on Precision Agriculture, Bloomington, MN, USA, 16–19 July 2000.

272. McCormick, S.; Bailey, J.S.; Jordan, C.; Higgins, A. A potential role for electrical conductivity mapping in the site-specific management of grassland, *Centre Agricult. Landscape Land Use Res.* **2003**, 393.

273. Oliver, Y.M.; Wong, M.T.F.; Robertson, M.J. Targeting the subsoil to better manage acidity spatially. In Proceedings of the 17th ASA conference, Hobart, Australia, 20–24 September 2015. Available online: http://2015.agronomyconference.com/papers/agronomy2015final00049.pdf (accessed on 1 November 2017).

274. Proffitt, T.; Bramley, R. Further developments in precision viticulture and the use of spatial information in Australian vineyards. *Aust. Vitic.* **2010**, *14*, 31–39.

275. Robinson, N.J.; Rampant, P.C.; Callinan, A.P.L.; Rab, M.A.; Fisher, P.D. Advances in precision agriculture in south-eastern Australia. II. Spatio-temporal prediction of crop yield using terrain derivatives and proximally sensed data. *Crop Pasture Sci.* **2009**, *60*, 859–869.

276. Saleh, A.; Belal, A.A. Delineation of site-specific management zones by fuzzy clustering of soil and topographic attributes: A case study of East Nile Delta, Egypt. *IOP Conf. Ser.: Earth Environ. Sci.* **2014**, *18*, 012046.

277. Schepers, A.R.; Shanahan, J.F.; Liebig, M.A.; Schepers, J.S.; Johnson, S.H.; Luchiari, A. Appropriateness of management zones for characterizing spatial variability of soil properties and irrigated corn yields across years. *Agron. J.* **2004**, *96*, 195–203.

278. Sun, Y.; Cheng, Q.; Lin, J.; Schellberg, J.; Schulze Lammers, P. Investigating soil physical properties and yield response in a grassland field using a dual-sensor penetrometer and EM38. *J. Plant Nutr. Soil Sci.* **2013**, *176*, 209–216.

279. Türker, U.; Talebpour, B, Yegül, U. Determination of the relationship between apparent soil electrical conductivity with pomological properties and yield in different apple varieties. *Žemdirbystė-Agriculture* **2011**, *98, 307–314*.

280. Karl Vanderlinden, G.M. Juan Vicente Giráldez, José Luis Muriel, Characterizing Soil Management Systems using Electromagnetic Induction. In Proceedings of the 19th World Congress of Soil Science, Soil Solutions for a Changing World, Brisbane, Australia, 1–6 August 2010.

281. Vitharana, U.W.A.; Van Meirvenne, M.; Simpson, D.; Cockx, L.; De Baerdemaeker, J. Key soil and topographic properties to delineate potential management classes for precision agriculture in the European loess area. *Geoderma* **2008**, *143*, 206–215.

282. Zhang, R.; Wienhold, B.J. The effect of soil moisture on mineral nitrogen, soil electrical conductivity, and pH. *Nutr. Cycl. Agroecosyst.* **2002**, *63*, 251–254.

283. McBratney, A.; Gruijter, J.D. A continuum approach to soil classification by modified fuzzy k-means with extragrades. *Eur. J. Soil Sci.* **1992**, *43*, 159–175.

284. Corwin, D.; Carrillo, M.; Vaughan, P.; Rhoades, J.; Cone, D. Evaluation of a GIS-linked model of salt loading to groundwater. *J. Environ. Qual.* **1999**, *28*, 471–480.

285. Kitchen, N.R.; Sudduth, K.A.; Myers, D.B.; Drummond, S.T.; Hong, S.Y. Delineating productivity zones on claypan soil fields using apparent soil electrical conductivity. *Comput. Electron. Agric.* **2005**, *46*, 285–308.

286. Abuzar, M.; Rampant, P.; Fisher, P. Measuring spatial variability of crops and soils at sub-paddock scale using remote sensing technologies. In Proceedings of the 2004 IEEE International Geoscience and Remote Sensing Symposium, Anchorage, AK, USA, 20–24 September 2004; pp. 1633–1636.

287. Kravchenko, A.N.; Harrigan, T.M.; Bailey, B.B. Soil Electrical Conductivity as a Covariate to Improve the Efficiency of Field Experiments. *Trans. ASAE* **2005**, *48*, 1353–1357.

288. Lawes, R.A.; Bramley, R.G.V. A Simple Method for the Analysis of On-Farm Strip Trials. *Agron. J.* **2012**, *104*, 371–377.

289. Kravchenko, A.N.; Robertson, G.P.; Thelen, K.D.; Harwood, R.R. Management, Topographical, and Weather Effects on Spatial Variability of Crop Grain Yields. *Agron. J.* **2005**, *97*, 514–523.

290. Cosby, A.; Trotter, M.; Falzon, G.; Stanley, J.; Powell, K.; Schneider, D.; Lamb, D. Mapping redheaded cockchafer infestations in pastures—Are PA tools up to the job? In *Precision Agriculture'13*; Wageningen Academic Publishers: Wageningen, The Netherlands, 2013; pp. 585–592.

291. Hbirkou, C.; Welp, G.; Rehbein, K.; Hillnhütter, C.; Daub, M.; Oliver, M.; Pätzold, S. The effect of soil heterogeneity on the spatial distribution of Heterodera schachtii within sugar beet fields. *Appl. Soil Ecol.* **2011**, *51*, 25–34.

292. Jaynes, D.B.; Novak, J.M.; Moorman, T.B.; Cambardella, C. Estimating herbicide partition coefficients from electromagnetic induction measurements. *J. Environ. Qual.* **1995**, *24*, 36–41.

293. Olesen, J.E.; Jørgensen, L.N.; Jensen, P.K.; Thomsen, A.G.; Jensen, J.E. Sensor-Based Graduation of Fungicide Application in Winter Wheat. Available online: https://www2.mst.dk/udgiv/publications/2008/978-87-7052-701-9/pdf/978-87-7052-702-6.pdf (accessed on 1 November 2017).

294. Ritter, C.; Dicke, D.; Weis, M.; Oebel, H.; Piepho, H.P.; Büchse, A.; Gerhards, R. An on-farm approach to quantify yield variation and to derive decision rules for site-specific weed management. *Precis. Agric.* **2008**, *9*, 133–146.

295. Bevan, B. The search for graves. *Geophysics* **1991**, *56*, 1310–1319.

296. Dalan, R.A.; Bevan, B.W. Geophysical indicators of culturally emplaced soils and sediments. *Geoarchaeol. Int. J.* **2002**, *17*, 779–810.

297. Dalan, R.A. Remote Sensing in Archaeology: An Explicitly North American Perspective. In *Magnetic Susceptibility*; Johnson, J.K., Ed.; University of Alabama Press: Tuscaloosa, AL, USA, 2006; pp. 161–203.

298. Ferguson, R.B. The search for port la joye: Archaeology at Ile Saint-Jeans first French settlement. *Island Mag.* 1990, 27, 3–8.

299. Santos, V.R.N.; Porsani, J.L.; Mendonça, C.A.; Rodrigues, S.I.; DeBlasis, P.D. Reduction of topography effect in inductive electromagnetic profiles: Application on coastal sambaqui (shell mound) archaeological site in Santa Catarina state, Brazil. *J. Archaeol. Sci.* **2009**, *36*, 2089–2095.

300. Simpson, D.; Lehouck, A.; Verdonck, L.; Vermeersch, H.; Van Meirvenne, M.; Bourgeois, J.; Thoen, E.; Docter, R. Comparison between electromagnetic induction and fluxgate gradiometer measurements on the buried remains of a 17th century castle. *J. Appl. Geophys.* **2009**, *68*, 294–300.

301. Simpson, D.; Lehouck, A.; Van Meirvenne, M.; Bourgeois, J.; Thoen, E.; Vervloet, J. Geoarchaeological prospection of a Medieval manor in the Dutch polders using an electromagnetic induction sensor in combination with soil augerings. *Geoarchaeol.—Int. J.* **2008**, *23*, 305–319.

302. Viberg, A.; Trinks, I.; Lidén, K. *Archaeological Prospection in the Swedish Mountain Tundra Region*; Presses Universitaires de Rennes: Rennes, France, 2009.

303. Bevan, B.W. The Search for Graves. *Geophysics* **1991**, *56*, 1310–1319.

304. McNeill, J.D. The application of electromagnetic techniques to environmental geophysical surveys. *Geol. Soc. Lond. Eng. Geol. Spec. Publ.* **1997**, *12*, 103–112.

305. Sharma, D.P.; Gupta, S.K. Application of EM38 for Soil Salinity Appraisal: An Indian Experience. Available online: http://content.alterra.wur.nl/Internet/webdocs/ilri-publicaties/special_reports/Srep13/Srep13-h3.pdf (accessed on 1 November 2017).